

FROM SEA TO SURGERIES, FROM BABBLING BROOKS TO BABY SCANS: BUBBLE ACOUSTICS AT ISVR

TG Leighton Institute of Sound and Vibration Research, University of Southampton, Highfield, Southampton SO17 1BJ, UK

1 INTRODUCTION

Ultrasound is passed through liquids and tissue both for diagnostic reasons, and in order to produce a material change. The most familiar diagnostic application is the external foetal scanning that is routine in many pregnancies. However many more sites are now benefiting from ultrasonic scanning. This is evidenced by the presence of probes for use whilst inserted into the vagina, rectum and oesophagus; and the increase in the maximum insonification frequency from 30 MHz to one of 80 MHz, for use on shallow sites in dermatological and ophthalmometric work (where enhanced spatial resolution is required, but the increased absorption at these frequencies is not debilitating). Even in foetal scanning, new techniques are being explored (Figure 1) with, for example, the use of small bubbles to act as contrast agents¹. Non-imaging diagnostic methods have also developed, for example in the use of ultrasound to investigate bone health and osteoporosis²⁻⁴.

Acoustic methods are however exploited for diagnostic purposes outside of biomedicine. In addition to the military uses, environmental applications in the ocean alone^{5,6} include: Propagation of signals over 1000 km in feasibility studies for monitoring global warming⁷; and monitoring sediment transport down large rivers^{8,9}, a parameter key to land fertility and sonar operation in coastal waters. Both developed from initial research for military applications¹⁰⁻¹⁵, a common theme: In the seabed alone, mine detection^{16,17} has produced benefits for communications (Figure 2) and geological surveying^{18,19} (Figure 3) with beneficiaries ranging from the petrochemical industry to marine archaeology²⁰.

In liquids, the most acoustically active naturally-occurring entities are gas bubbles. Figures 1 and 3 illustrate this, in that the strongest echoes in both images are from bubbles. The characterisation of bubble populations in acoustical oceanography is not only promoted by their potency in affecting sound fields, but also by their importance to environmentally significant processes: Coastal erosion and wave dynamics²¹⁻²⁵; methane seeps²⁶; and the flux between the ocean and atmosphere of momentum, energy and mass²⁷. The top 2.5 m of the ocean has a heat capacity equivalent to the entire atmosphere; and the flux²⁸ between atmosphere and ocean of carbon alone exceeds 10⁹ tonnes/year. Section 2 will discuss techniques for diagnosing bubble populations.

Given the exceptionally efficient coupling between bubbles and acoustic waves which Figures 1 and 3 demonstrate, it is perhaps not surprising that the potency of bubbles in acoustics is by no mean restricted to diagnosis. In 1917 Lord Rayleigh identified the energetic bubble collapse known as 'cavitation' as being the cause of the propeller failure which had been plaguing ships²⁹. The ability of bubbles to process the materials which make them up and surround them will be discussed in Section 3.

2 ACOUSTIC BUBBLES IN DIAGNOSIS

The first measurements³⁰ of the size distribution of bubble population in the natural world using the passive acoustic emission were made in 1985. The technique of inferring bubble radii in the natural world from the natural frequencies they emit (Figure 4), has since given rise to hundreds of studies^{5,6,31}, from rainfall sensing^{32,33}, to industrial sparging^{1,34}, to extra-terrestrial studies (Figure 5). Development of this technique included innovative use of the Gabor Transform^{33,35} and spectral methods for when entrainment rates are high³¹. Whilst the bubble wall can undergo a variety of modes of oscillation³⁶, with some exceptions³⁷⁻⁴⁰ it is the pulsation which is the most acoustically

active, generating a strong monopole emission. Having natural frequencies inversely proportional to their radii, the typical oceanic air bubble population (having radii ranging from millimetres to microns) provide pulsation natural frequencies in the frequency range of at least 1-500 kHz respectively, with commensurate quality factors of roughly 30 to 5. Emitting so potently in this range when entrained, they provide sound sources in passive sonar systems (which may represent unwanted noise or a desirable source, e.g. in locating a vessel or in 'acoustic daylight' systems⁴¹).

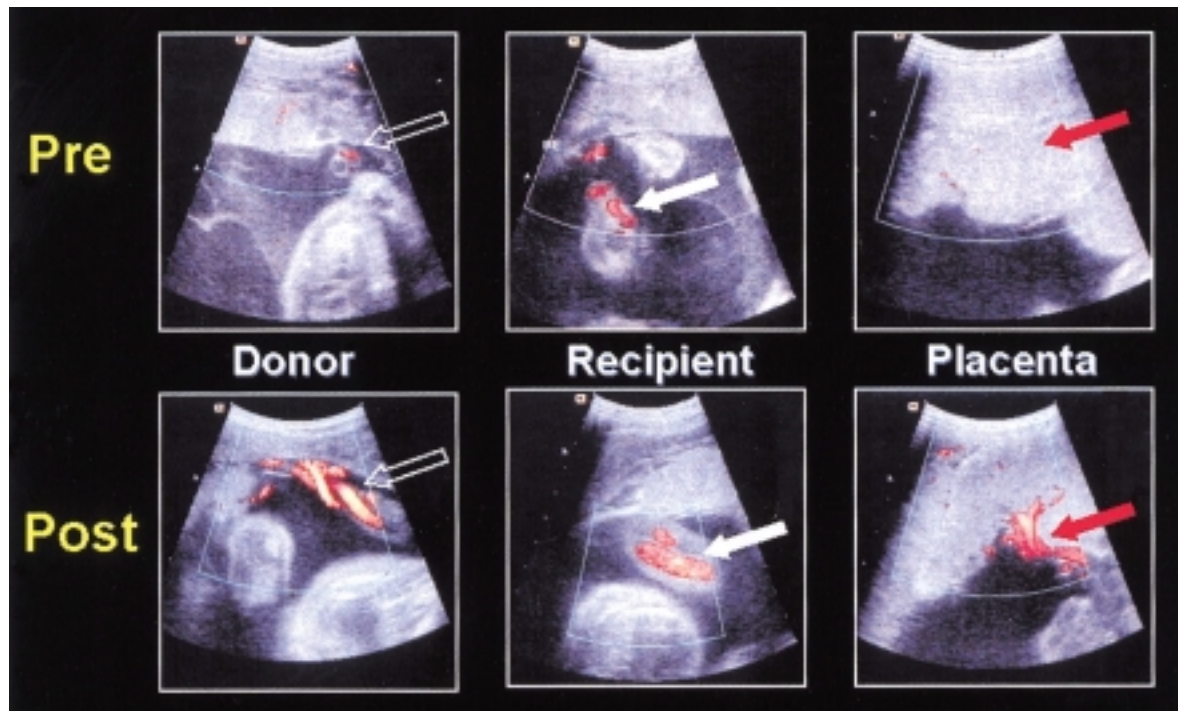


Figure 1. In 20% of cases where a single chorionic membrane surrounds both twins (i.e. monochorionic), vascular connections between the twins via the placenta are virtually omnipresent, which allows inter-fetal blood transfusion as a normal event. However in 15% of such cases an imbalance occurs, leading to Twin-twin transfusion syndrome. If left untreated, this has over 80% mortality (with complications present in some survivors). The ultrasonic imaging of blood flow can be greatly enhanced by ultrasonic contrast agents (UCA), which usually take the form of microscopic gas bubbles that are injected into the bloodstream. If UCA is injected into one twin, and subsequently appears in the bloodstream of the other twin, inter-twin transfusion has been diagnosed and the donor/recipient roles identified. If it were possible to identify the blood vessel in the placenta which is responsible for the transfer, it could be sealed, saving both twins. The figure shows Power Doppler ultrasonic images before (top row) and after (bottom row) the injection of a commercial bubble-based UCA (SH U 508A) into the donor of a monochorionic twin pair. A threshold is preset: Echo strengths from UCA exceed this, and are coloured red (although occasional returns which exceed the threshold in the absence of UCA are possible, as seen in the top row). In each case, the images show signal enhancements attributable to the contrast agent during maintenance of constant ultrasonic parameters. Left: Cross section through the first (Donor) twin's cord (arrow) before (top) and after (bottom) the administration of contrast agent. Middle: cross section through the contralateral (Recipient) twin's cord (arrow) before (top) and after (bottom) inter-fetal transfusion of contrast agent. Right: Placental appearance (arrow) before (top) and after (bottom) injection of contrast agent. Reproduced with permission from Denbow et al.⁴².

It is through this pulsation mode that bubbles undertake their acoustic resonance. This has been exploited in numerous systems for bubble detection⁴³ in industry, biomedicine and the oceans. Indeed, the studies have extended from bubbles in free fields to bubbles in tubes (including ear canals and blood vessels)^{44,45} and in pipes⁴⁶, where the crucial correction for reverberation⁴⁷ to the free fields theory that had been used for decades was shown to remove errors of up to a ~100% in previous inversions of acoustic data to determine bubble populations.

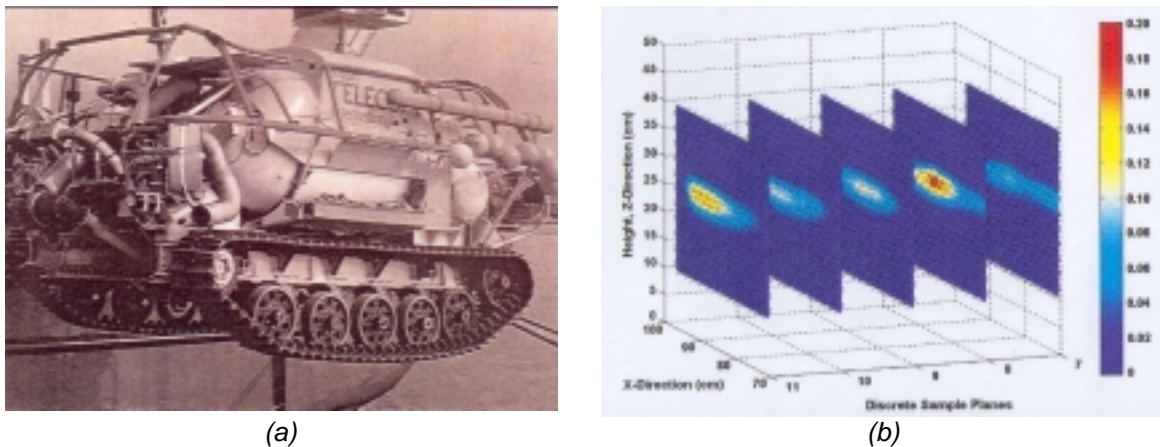


Figure 2. (a) The 3 metre long 'Seadog' underwater vehicle is used for the burial, tracking and repair of optical fibre telecommunications cables. It operates at a maximum sea depth of 275 m (from ROV Review 1993-4, WAVES magazine, Windate Enterprises Inc., 5th edition). The current generation of optical fibre telecommunications cables contain metal components, which enables such vehicles to locate cables buried in seabed using magnetometers. The next generation of cables will not contain metal, and hence cannot be located using magnetometers if, for example, they need repair. (b) Acoustic detection of the next generation of cables is not simple, because of the similarity in acoustic impedance between optical fibre and sediment. However research at ISVR has developed an acoustic solution, and parallel image planes through sediment clearly reveal the location of a non-metallic cable (R.C.P. Evans and T.G. Leighton)^{48,49}.

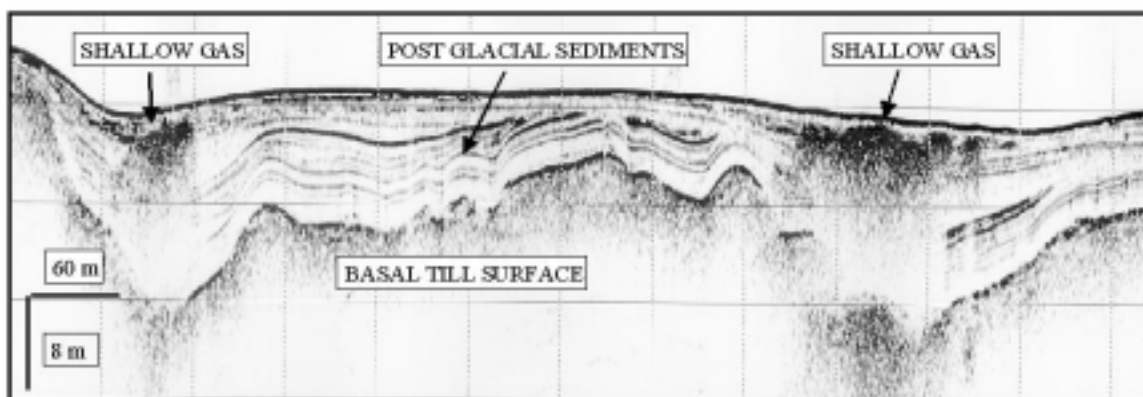


Figure 3. Shallow gas deposits in the underwater sediment of Strangford Lough, Northern Ireland. Reproduced by permission of Southampton Oceanography Centre (J.K. Dix, J. Bull and J.S. Lenham).

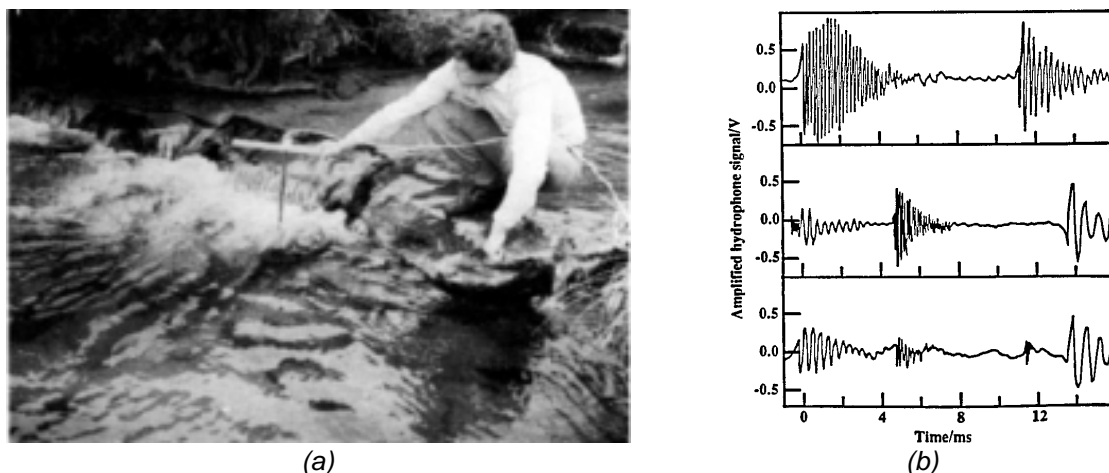


Figure 4. (a) The author (age 21) at Kinder Scout in the Peak District (Derbyshire, UK). (b) Three selections from the hydrophone sound recording made at site (a). Each exponentially decaying sinusoid indicates the bubble source is a lightly damped oscillator, the radius of which can be determined from the natural frequency. Here the counting of bubbles is made simple because the low entrainment rate means there is little overlap between bubble signatures. From Leighton and Walton³⁰.

The bubble is however a nonlinear oscillator, and the generation of higher harmonics has been an invaluable tool in separating out the strong echoes or attenuation which results from pulsation resonance, from similar effects which simply result from much larger off-resonance bubbles. When the bubble population is very dense, such ambiguities hinder the use of the pulsation resonance as a method of determining the bubble size. Therefore for example in the world's first measurements⁵⁰ of the bubble size distribution in the surf zone (Figure 6), a nonlinear combination-frequency technique had to be used. Two years later, in 1998, the same technique provided the first time-resolved measurements of oceanic bubble population⁵¹; this was followed in 2001 by the first measurement of a bubble size distribution in the surf zone under windspeeds of 50 mph (Figure 7)⁵². However the bubble nonlinearity goes beyond a simple quadratic term which might generate second harmonics or combination frequencies⁵³: Subharmonics can be generated; and the most precise^{54,55} technique for the measurement of the size of a single bubble arose from the discovery⁵⁶ of the generation of signals at $\omega_i \pm \omega_p / 2$ when a bubble is insonified by a high frequency imaging signal (at frequency ω_i) and a lower frequency 'pump' signal (at frequency ω_p which is tuned to coincide with the bubble pulsation resonance). The mechanism responsible for this was discovered⁵⁷⁻⁵⁹ to be the generation of Faraday waves upon the bubble walls.

Other novel methods for characterisation of bubble clouds include the use of Higher Order Statistics⁶⁰⁻⁶³, and the first only (to date) deployment of acoustoelectrochemical techniques at sea⁶⁴. To counteract the ambiguities in any individual technique when employed in such challenging environments, the principle of using multiple techniques to counterbalance the limitations and ambiguities inherent in one technique was proposed^{54,55,65}, along with a scheme for assessing the invasiveness of any individual technique⁶⁶.

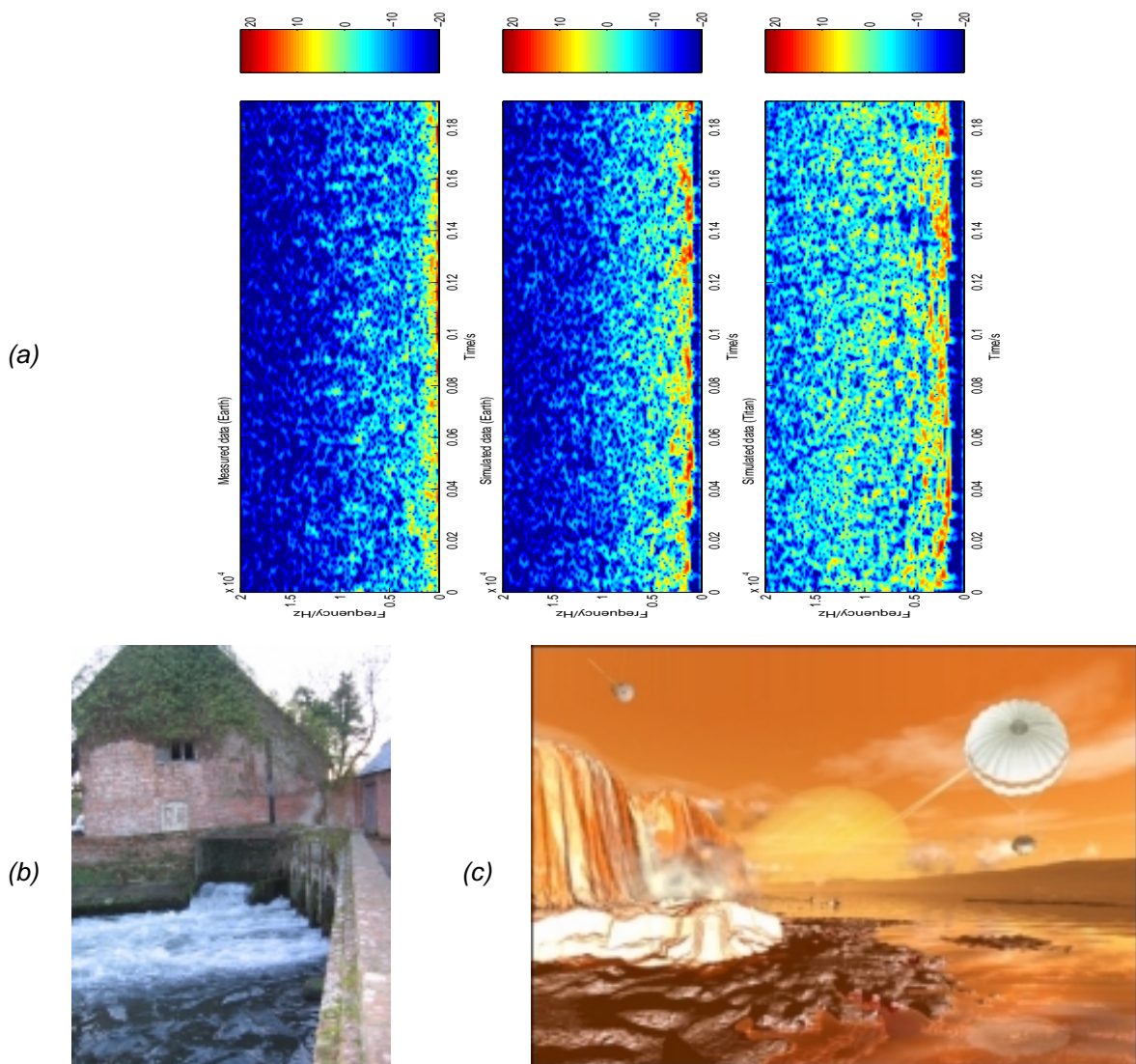


Figure 5. (a) Compared with Figure 4b, the individual bubbles signatures cannot readily be distinguished in hydrophone data taken in Sadler's Mill Romsey (Figure 5b) in the spectrogram on the left of Figure 5a. Nevertheless it is possible to estimate a bubble size distribution from this¹. From the statistics of that bubble size distribution¹, it is possible to reconstruct the spectrogram for Sadler's Mill (Figure 5a, middle plot). This has a power spectra close to the original¹. Inputting the data relevant to Titan, it is possible to predict sound (Figure 5a, right plot) from a methane-fall (seen on the left of Figure 5c falling into an ethane lake) if it produces a bubble population with the same statistics. Titan will be visited by the Cassini-Huygens mission in 2004: Figure 5c shows the Huygens probe parachuting through Titan's atmosphere, having previously detached from the Cassini vehicle (seen in the upper left of the image). Thin methane clouds dot the horizon, and methane vapour is generated by the methane-fall. It, and rain based on a methane/ethane evaporation/condensation cycle, fall in a surface gravity which is approximately $1/10^{\text{th}}$ that of Earth, although the extreme cold (surface temperature 93 K) contributes to a surface atmospheric pressure of 1.6 times that of Earth. Smooth ice features rise out of the methane/ethane lake, and crater walls can be seen far in the distance. Given the myriad uses for diagnosis by bubble-generated sound on Earth, from rainfall sensing to atmosphere/ocean mass flux, its use as an extraterrestrial diagnostic presents intriguing possibilities, particularly because of the low power and hardware requirements of this passive system. (Painting by D. Seal; Credit: NASA/JPL/Caltech. Spectrograms by P.R. White and T.G. Leighton: The dB colour scale has the same reference for all three. These recordings can be heard via the 'Research' page at <http://www.isvr.soton.ac.uk/fdag/UUA/index.htm>).



Figure 6. The first measurement of the bubble size distribution in the surf zone (at Hull). The acoustic detector is the small black circle clamped between the two smaller uprights. The wave measures approximately 10 feet tall. Taken from Leighton et al.⁵⁰



(a)



(b)

Figure 7. Two photographs, taken a fraction of a second apart, showing (a) two of the author's PhD students (S.D. Meers and M.D. Simpson) attempting to bolt sensors to a scaffolding rig the team have just deployed at sea; (b) Mr Simpson's feet (Mr Meers is not visible). During the subsequent trial the winds increased from the calm conditions shown here to speeds in excess of 50 mph. Taken from Leighton et al.⁸³.

It should be noted^{1,83} that the bubble populations measured by the passive techniques of Figures 4 and 5, differ from the populations measured by the active techniques of the preceding paragraph, where the bubble population is insonified by an external sound field. Passive emissions come only from those bubbles which are actively 'ringing'. This occurs only within the first few milliseconds after entrainment for most bubbles. Inversion of passive acoustic emissions will therefore estimate the population size distribution of 'ringing' bubbles. Optical and active acoustic techniques actually

measure the size distribution of a different bubble population, comprising not only the ringing bubbles but also the silent bubbles which have ceased to emit passively, but which nevertheless persist in the water column. In 2001 it was first proposed⁶⁷ that, by comparing the results of active and passive measurements, one might learn about the processes which occur beneath a breaking wave (such as turbulence, circulation, buoyancy, etc. – Figure 8). These processes convert the population initially produced by the breaking wave (the one measured by the passive acoustic technique) into the background population (as measured by the active acoustic technique). One process not included in this is bubble fragmentation, although the same research programme did see the only testing to date of the relevant theory for this process^{33,35}.

Probably the most popular technique for the active acoustic measurement of bubble populations is through monitoring the sound speed and attenuation of an acoustic signal as it propagates between two points⁶⁸. The effects of bubbles on the sound speed have been known for some time⁶⁹: If the bubbles are driven in stiffness mode, they tend to reduce the sound speed. Even in the quasi-static conditions attained at the lowest frequencies, there is a finite reduction in the sound speed. If they are driven in inertia-controlled mode, they tend to increase the sound speed, the effect disappearing at the highest frequencies. The effects tend to increase as one approaches resonance.

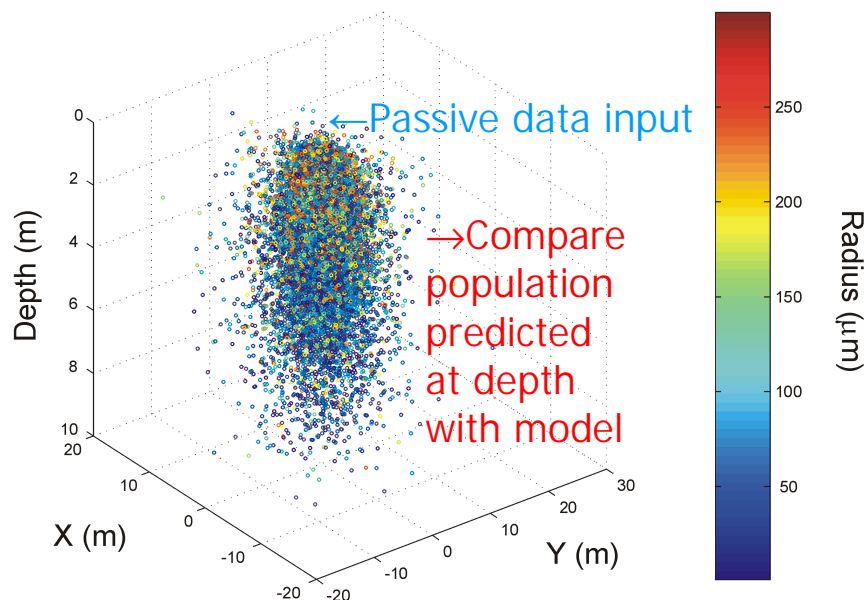


Figure 8. A single frame from an animation by M. D. Simpson and T. G. Leighton (similar ones are available via 'Research' at <http://www.isvr.soton.ac.uk/fdag/UUA/index.htm>). The air/sea interface is flat and at depth 0 m; the seabed is flat and at depth 10 m. Into a 3D section of ocean measuring 40 m x 50 m x 10 m deep is injected a bubble population. This 'entrainment' population is based on measurements of the passive noise from breaking waves, and the bubbles are introduced at the origin. The population then evolves under the influence of buoyancy, turbulence, surface tension and hydrostatic pressure, and gas flux occurs as for example the bubbles dissolve. The frame shows the bubble cloud about 30 s after injection. The bubble size distribution is colour coded, and it is for example clear that whilst turbulence has dispersed the cloud spatially, both buoyancy and hydrostatic effects result in the tendency for small bubbles (blue) at depth, with the larger (yellow/orange/red) bubbles tending to occur only close to the surface. The accuracy of such models were investigated⁶⁷ by comparing the predicted bubble population as a function of depth with the measurements of active acoustic techniques, such as those described in this paper. Each of the 64000 bubbles in the simulation must represent approximately 10^4 bubbles in nature

A fanciful speculation on one possible implication of this is found in a novel hypothesis⁷⁰ which might explain the mystery of the mechanism by which humpback whales (*Megaptera novaeangliae*) exploit bubble nets to catch fish.

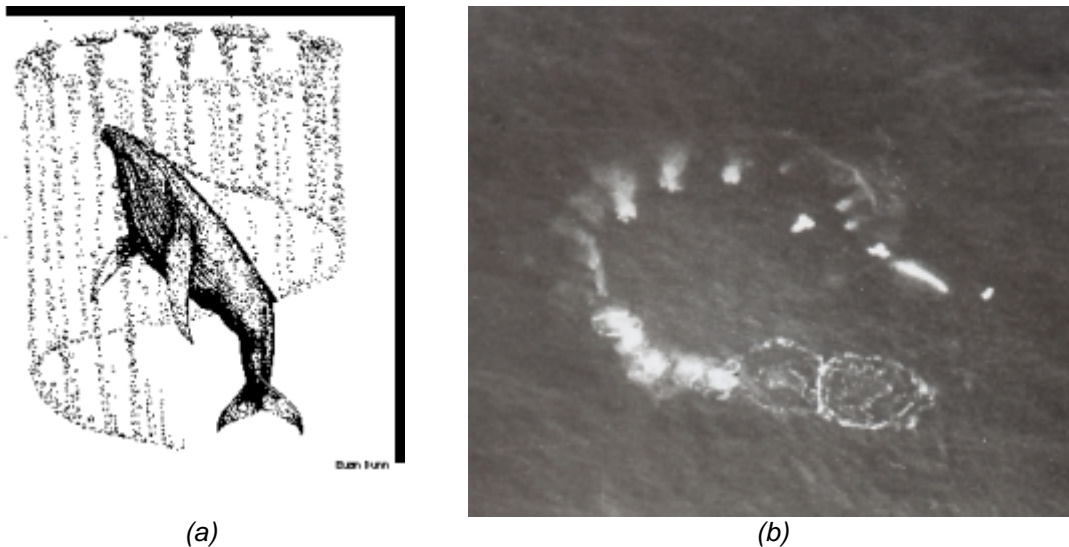
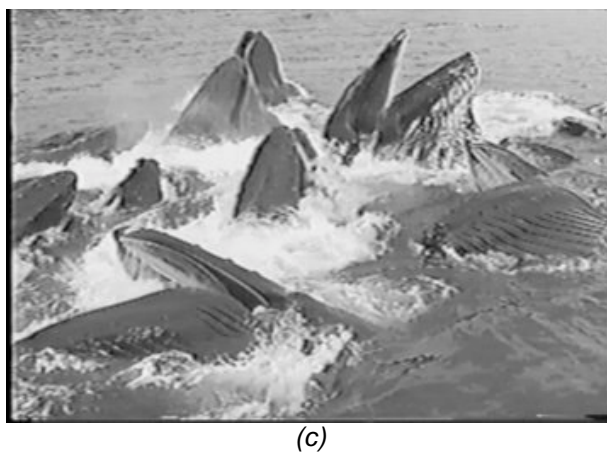


Figure 9. (a) Schematic of a humpback whale creating a bubble net. A whale dives beneath a shoal of prey and slowly begins to spiral upwards, blowing bubbles as it does so, creating a hollow-cored cylindrical bubble net. The prey tend to congregate in the centre of the cylinder, which is relatively free of bubbles. Then the whale dives beneath the shoal, and swims up through the bubble-net with its mouth open to consume the prey ('lunge feeding'). Groups of whales may do this cooperatively (Image courtesy of Cetacea.org). (b) Aerial view of a humpback bubble net (photograph by A. Brayton, reproduced from reference 71. (c) Humpback whales lunge feeding (Image courtesy of L. Walker, <http://www.groovedwhale.com>).



It has been known for decades that up to 30 whales might dive deep and then release bubbles to form the walls of a cylinder, the interior of which is relatively bubble-free (Figure 9a,b)⁷². The prey are trapped within this cylinder, for reasons previously unknown, before the whales lunge feed on them from below (Figure 9c). When the whales form such nets, they emit very loud, 'trumpeting feeding calls', the available recordings⁷³ containing energy up to at least 4 kHz. A suitable void fraction profile would cause the wall to act as a waveguide. Assume the scales permit the use of ray representation. Figure 10 shows how, with tangential[†] insonification, the mammals could generate a 'wall of sound' around the net, and a quiet region within it. If the fish approach the walls, they become startled by the intense sound (which may not only be subjectively loud, but also affect the

[†] Even if the whales do not create sufficiently directional beams and insonify tangentially, the bubble net might still function through its acoustical effects. The 'wall of sound' effect in Figure 10b is generated from those rays which impact the wall at low grazing angles. Those rays which never impact the wall do not contribute to the 'wall of sound'. If rays of higher grazing angle impact the net, they may cross into the net interior, though their amplitudes would be reduced by the bubble scattering, and attenuation alone would generate a quieter region in the centre of the net.

swim bladder, a resonant system). The natural schooling response of fish to startling would, in the bubble net, be transformed from a survival response into one that aids the predator in feeding.

Figure 10b plots the raypaths (calculated using standard techniques⁷⁴) from four whales for the stated launch conditions, for a bubble net in which the void fraction increases linearly from zero at the inner and outer walls, to 0.01% at the mid-line of the wall.

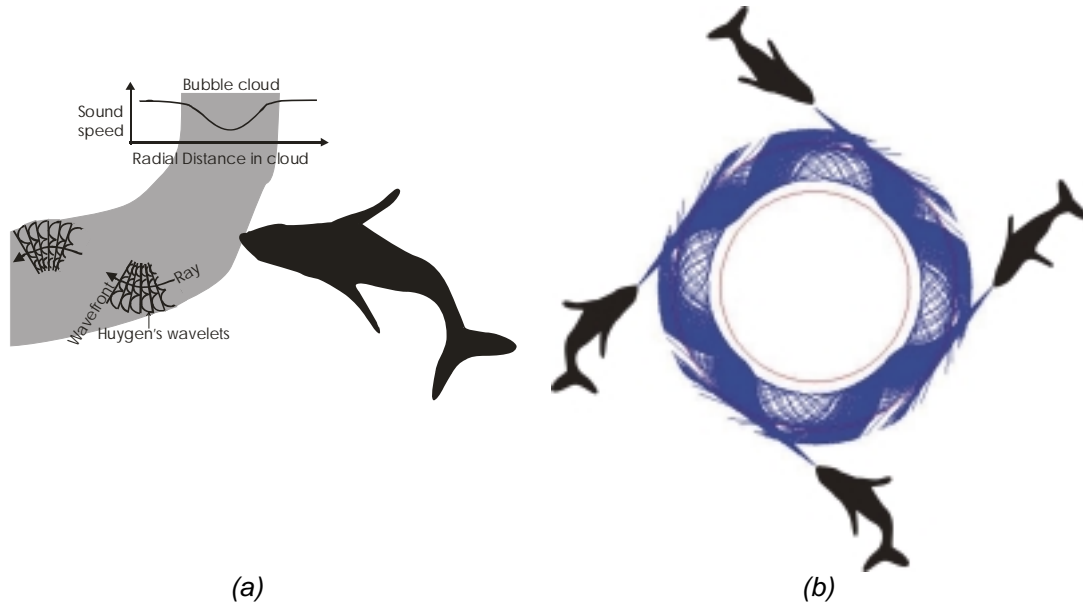


Figure 10 (a) Schematic of a whale insonifying a bubble-net (plan view), illustrating the sound speed profile in the cloud and, by Huygen's construction, sample ray paths. The sound speed profile assumes void fractions are greatest in the mid-line of the net wall, and assumes that the bubbles pulsate in stiffness mode. Hence the closer a Huygens wavelet is to the mid-line, the smaller the radius of the semicircle it forward-plots in a given time. Rays tend to refract towards the mid-line. (b) Four whales insonify an annular bubble net, where the bubbles are driven in stiffness-controlled mode such that the sound speed decreases linearly from being zero at the walls to 750 m/s at the cloud midline. The rays are coloured blue, and the locations of the inner and outer walls of the net are shown in red. Computed ray paths, where each whale launches 281 rays with an angular extent of 10° , refract as in (a). The rays gradually leak out, although some rays can propagate around the entire circumference. Plotting of a raypath is terminated when it is in isovelocity water and on a straight-line course which will not intersect the cloud. This refers to rays whose launch angles are such that they never intersect the net; and to rays which, having entered the net and undertaken two or more traverses of the mid-line, leave it. (c) Example ray paths computed for a cloud where the bubbles are driven in inertia-controlled mode such that the sound speed increases linearly from being zero at the walls to 2200 m/s at the cloud midline. The rays are coloured blue, and the locations of the inner and outer walls of the net are shown in red. For this simulation, however, the single source has a 45° beamwidth in order to illustrate the variety of ray bending that is possible (a 10° beam, as used in Figure 10b, tends to cause all rays follow a similar path, either traversing the net or refracting out of it, depending on the angle with which it intercepts the outer wall of the net). (Figures from T. G. Leighton, S. D. Richards and P. R. White)⁷⁰.

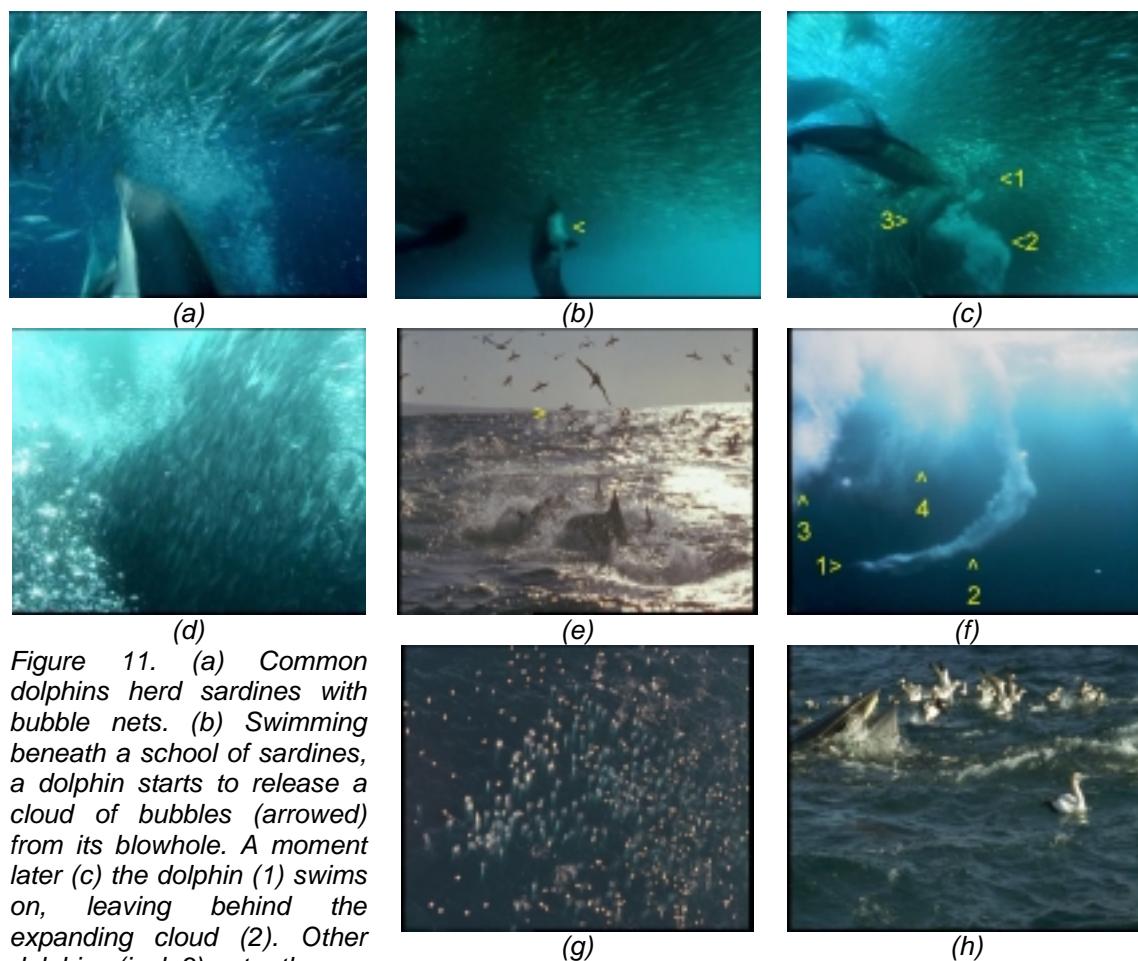


Figure 11. (a) Common dolphins herd sardines with bubble nets. (b) Swimming beneath a school of sardines, a dolphin starts to release a cloud of bubbles (arrowed) from its blowhole. A moment later (c) the dolphin (1) swims on, leaving behind the expanding cloud (2). Other dolphins (incl. 3) enter the frame. (d) The sardines school within a surrounding wall of bubbles that they are reluctant to cross, whilst (e) gannets dive into the sardine shoal to feed, folding their wings just before entry (arrowed). Dolphins are visible in the foreground. (f) On diving, a gannet (1) entrains a bubble plume (2). Plumes a few seconds old (3, with an older 4) have spread. (g) An aerial view shows hundreds of tight bubble plumes beneath airborne gannets. (h) A Bryde's Whale joins the feed. It surfaces with open mouth, which it then closes, sardines spilling from it. Images courtesy The Blue Planet (BBC, Discovery). See Byatt et al.⁸⁰

The actual acoustics of the cloud will of course be complicated by 3D effects and the possibility of collective oscillations; and even, speculatively, bubble-enhanced parametric sonar effects³⁶ which might be utilized by whales, for example to reduce beamwidth or generate harmonics, sum- and difference-frequencies etc..

The effect follows the frequency dependency described above. At frequencies sufficiently high to drive the bubble cloud in an inertia-controlled fashion, the bubbles produce an increase in sound speed. The wall is outwardly-refracting, and rays are no longer trapped within the cloud. The refractive effect of these bubbles on sound speed becomes negligible at even higher frequencies, although of course acoustic attenuation and scatter may be great. A variety of ray behaviour is possible^{1,70}, from reflecting straight off the net to traversing it and the interior with barely any refraction (Figure 10c). Such frequencies would not be effective in trapping prey, even if the prey could perceive them. However if scattering losses permit (and it is by no means certain they would), is it possible that, given these refracted paths, such frequencies could be used for echolocation of the contents of the net?

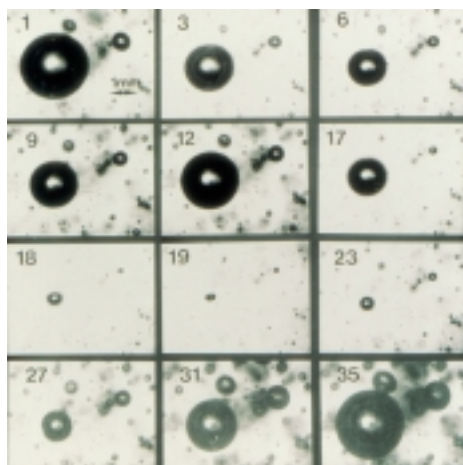


Figure 12. Nonlinear bubble pulsation in 100 Hz pressure field generated to the oscillation of a liquid column and filmed at 2000 fps. A selection of frames from the sequence of 35 consecutive frames show 1 period of the motion of stable air bubble oscillating in glycerol under a static pressure of 600 Pa, and oscillating pressure of 3900 Pa. The bubble contracts from maximum size in frame 1 to a minimum in frame 6, then expands to a second maximum (frame 12). It is then collapses to a second minimum (as frame 19) before expanding to the initial size. This cycle then repeats. The second collapse is gradual up to frame 17, but then becomes very rapid. Figure from Leighton et al.⁸².



(a)

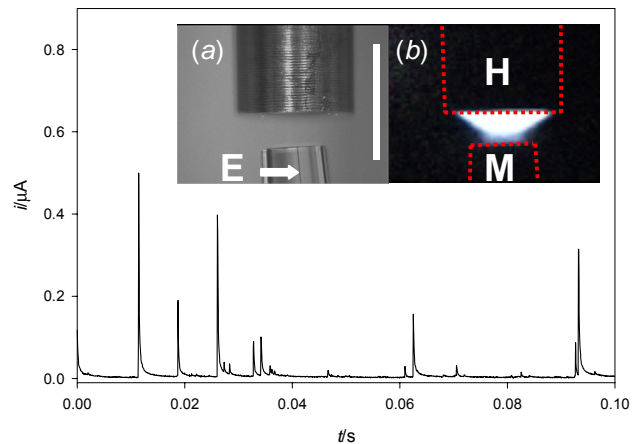


(b)

Figure 13 (a) An LUGM-145 (available for \$1900). It carries a 660kg charge, is based on a pre-First World War design, and is moored on a chain or drifts on the surface and is set off by contact with a ship. Modern mines are triggered by a ship's magnetic, acoustic or pressure signature (or combination of the above) so that they cannot readily be cleared by dummy contact methods. (b) Around \$5 million of damage was caused to the USS Tripoli (LPH-10) after it struck an LUGM-145 moored contact mine during operation Desert Storm. (DSTL were consulted before reproduction of this image.)

With humpbacks the probability appears to be low. Echolocation is normally associated with *odontoceti*, and although there are suggestions that humpbacks may exploit it^{75,76}, there is to date no evidence that they have used it to locate schools of prey. Although there is evidence of directionality in the songs of humpbacks^{77,78}, Figure 10b should not be interpreted as implying they can generate a 10° beam – we do not know one way or the other[†]. Similarly, the highest reported frequencies generated by humpbacks correspond to harmonics in recordings^{78,79} in excess of 15 kHz and 24 kHz, close to the bandwidth of the recording equipment. Exploitation of the inertia-controlled regime, as described above, would probably require higher frequencies. However dolphins have also been observed to feed using bubble net⁸⁰ (Figure 11a-d), and some can echolocate up to 200 kHz. It would perhaps be asking a lot for dolphins to identify fish amongst the strong bubble scatterers, although the environments which they naturally might encounter are similarly complex¹⁷. The prospect of trapping low frequency sound in a bubble cloud to herd prey (Figure 10b), whilst simultaneously echolocating with higher frequencies (Figure 10c), is attractive but perhaps unlikely.

Figure 14. Plot showing the current recorded as a function of time for a stainless steel microelectrode (25 μm diameter, marked E and surrounded by transparent insulation) exposed to inertial cavitation. Individual transients are caused by surface erosion as the result of inertial collapse. The inset images show the ultrasonic horn (H) positioned above a microelectrode (M) taken (a) in external illumination, and (b) with no external illumination. The scale bar represents 3 mm. The light in (b) shows in the image intensifier record of sonoluminescence. The position of the horn (H) and microelectrode (M) are indicated with dotted lines. (From P.R. Birkin, D. Offin and T.G. Leighton, *The study of surface processes under electrochemical control in the presence of inertial cavitation*, Submitted to *Wear* 2004).



It may however be that exploitation of the schooling of fish in response to startling using bubble acoustics is more widespread, if perhaps less elegant, than the scheme of Figure 10b. The filming associated with Byatt *et al.*⁸⁰ shows bubble plumes generated by gannets (Figure 11e-g) diving into a shoal of sardines which dolphins have herded to the sea surface. These plumes will no doubt complicate an underwater sound field already populated by the calls and bubble nets of dolphins, and the entrainment noise of the gannet bubble plumes, and could further stimulate the sardines to school. Gannets, dolphins, sharks and whales etc. (Figure 11h) all benefit from this, although to what extent this is intentional is unknown.

The linear theory for acoustic propagation through bubbly water has proved to be immensely successful, with the original paper⁸¹ being cited over 100 times. However bubble pulsations are inherently nonlinear^{1,82} (Figure 12), and this year sees the publication of the first theory for acoustic propagation through clouds in which the bubbles undertake nonlinear pulsations⁸³. This method builds on an earlier technique which combined nonlinear bubble dynamics with linear descriptions of dissipation⁸⁴. This work has resulted in the proposal and development of new techniques for the detection of mines in bubbly water (Figure 13), exploiting pulse-length dependence^{1,84,85} of scattering and attenuation, and the bubble nonlinearity^{1,86}. The importance of mine-hunting in modern warfare is very great. Since the start of the Cold War, at least fourteen U.S. ships have been damaged by mines, with some sinking. Mine clearance techniques include attempting to cause detonation by presenting the mine with a signal resembling that which its target would produce. To resist such attempts mines of considerable sophistication are being developed, which respond to the pressure, magnetic, underwater electric potential (UEP) and acoustic signatures of vessels (often in combination). However mines have a long operational lifetime, and simple contact devices produced decades earlier can be readily purchased, are inexpensive, and effective (Figure 13). In 1988 a simple contact mine costing \$1,500 (an Iranian SADAF-02) almost sank the *Samuel B. Roberts* (FFG-58) causing nearly \$96 million of damage. During the first Gulf War Iraq laid 1242 mines and, even though many were nonfunctional or ineffectively laid, three mines seriously damaged two U.S. warships, *Princeton* (CG-59) and *Tripoli* (Figure 13). These mines were laid in water 20-50 m deep.

In very shallow waters, mines might be much more successfully hidden by exploiting the bubble fields. There, the presence of mines presents a hazard to landing craft, for example, such that even without detonating the mine can seriously interfere with marine activity, which must be conducted cautiously. Sonar attempts to detect mines in very shallow water can fail, because the returned sonar signal can be dominated by the scatter from the wave-generated bubble clouds in the vicinity of the mine. Time-dependent and nonlinear techniques might enhance scatter from a mine and suppress that from the bubbles, aiding detection^{1,86}.

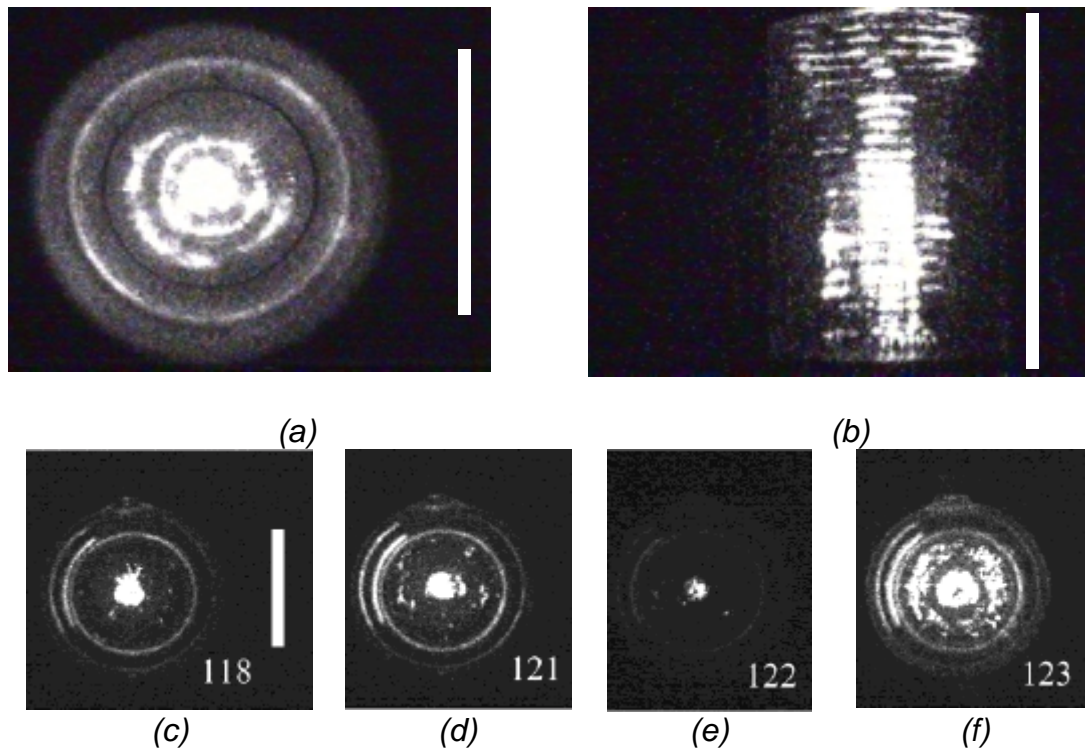
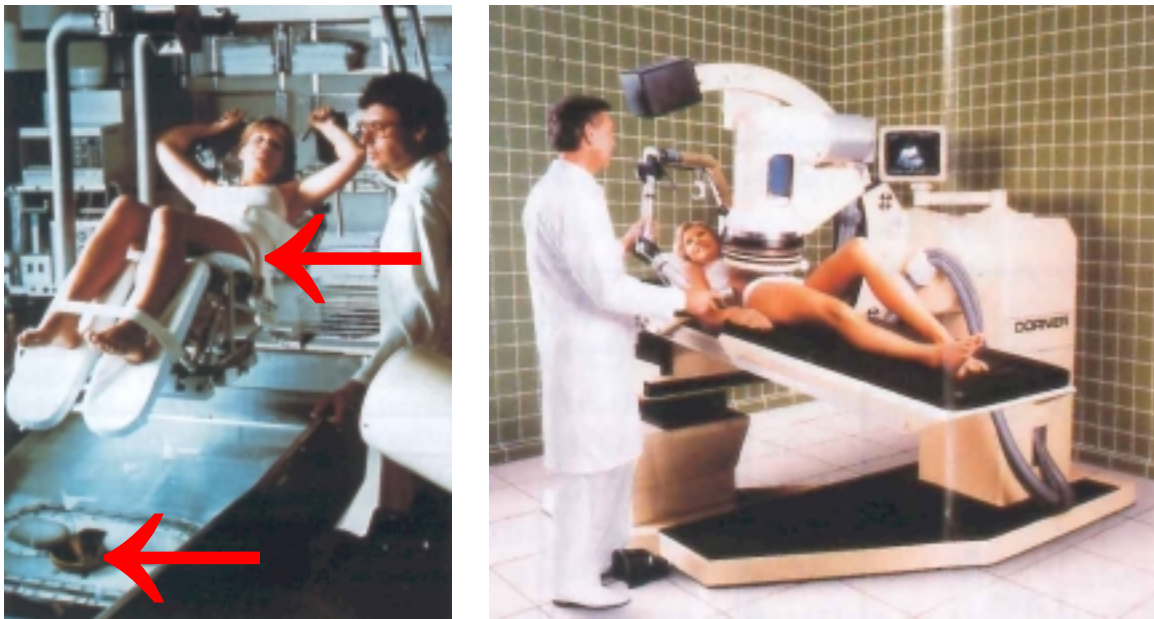


Figure 15. The acoustic pressure antinodes within reverberant water-filled cylinders (with vertical axis of symmetry, and the sound source at the cylinder base) are made visible through the chemiluminescence which occurs there. (a) Plan and (b) side views of luminescence (which occurs at pressure antinodes) in a water-filled cell which had a polymethylmethacrylate wall (9.4 cm internal diameter, 10 cm external diameter; height of aqueous solution=14 cm) for insonification at 132.44 kHz where the spatial peak acoustic pressure in the liquid was 0.75 bar. The scale bar in frame (a) represents 9.4 cm, while the scale bar in frame (b) represents 14 cm. Frames (c)-(f) (to which the scale bar of length 5.8 cm in frame (c) refers) were taken in a double-walled, water-jacketed cell (5.8 cm internal diameter, 8.5 cm external diameter, and liquid height 8 cm) which was maintained at a constant liquid temperature of 25°C. As the insonifying frequency changed, so too did the spatial peak acoustic pressure, providing the following combinations: (c) 118 kHz; 1.36 bar; (d) 121 kHz; 1.39 bar; (e) 122 kHz; 1.50 bar; (f) 123 kHz; 1.80 bar. The effect of tuning into particular acoustic modes is evident. By noting the modal resonance frequencies in these and similar cylinders, the sound speed in this bubbly water was found to be in the range 868-1063 m/s, implying void fractions of $2.9\text{-}4.2 \times 10^{-3} \%$. Frames selected from several figures in reference 125.

3 BUBBLE ACOUSTICS IN PROCESSING

As outlined in Section 1, Lord Rayleigh's 1917 publication²⁹ marked the beginning of a study of the ability of bubbles to process the material surrounding them. If such processing is desirable, it is most conveniently undertaken today through the use of ultrasonics (for example in a commercial ultrasonic cleaning bath⁸⁷). However, in that original 1917 case, violent bubble collapse was the result of hydrodynamic forces, and led to the erosion of a propeller blade. This phenomenon is still studied today, with for example the discovery of structure in the sonoluminescence emissions generated by cavitating flow over a hydrofoil⁸⁸. The newest techniques allow cavitation erosion to be monitored on the microsecond timescale (Figure 14), as opposed to the minute/hour timescales available only a decade ago. Specialised cavitation⁸⁹⁻⁹¹ systems have therefore allowed correlated monitoring of bubble wall motion, erosion, and luminescence in almost real-time⁹². This illustrates

the use of luminescence to indicate the spatial and temporal characteristics of cavitation which is capable of processing surrounding material. A spatial example can be found in the ability to generate sonoluminescence at the acoustic pressure antinodes of standing waves⁹³ (Figure 15). This facility enabled cavitation, located via its sonoluminescent emissions, to be correlated with cell death⁹⁴, which also occurred preferentially⁹⁵ at those antinodes compared to the nodes. Similarly, a temporal example provided data and new theories⁹⁶⁻¹⁰⁰ relating to the cavitation hazard (and its suppression) associated with pulsing the field. The pulsing characteristics of biomedical fields present a key component in designing and assessing the hazard associated with that field, although its relevance to the hyperthermia biohazard (tissue heating) has received more attention than its relevance to the risk of cavitation (whether unwanted¹⁰⁵ or desired¹⁰⁶).



(a)

(b)

Figure 16. (a) The original Dornier HM3 clinical lithotripter. Shock waves are focused onto kidney and gall stones to break them up. In this device, shock wave focusing relies on the principle that an ellipse has two foci. A submerged focusing reflector (lower arrow in the picture at the base of the bath) is made from the bottom half of an ellipse. The plane cutting the ellipse in half is horizontal and all points on it are equidistant between the two vertically-aligned foci. The shockwave is generated using a spark gap placed at the lower focus (through which ~20 kV is discharged). Therefore a spatial maximum in the acoustic pressure amplitude occurs at the upper focus of the ellipse (upper arrow), which should be steered to coincide with the location of the stone. This is done by lowering the patient into the waterbath, such that the water provides the necessary acoustic coupling. (b) The Dornier MPL9000 clinical lithotripter. The external electromagnetic shockwave source generates a planar wave that is focused on the target using an acoustic lens. The patient is not immersed: The shock is transmitted into the patient through a coupling "water unit" (such as a water cushion). The shock source and cushion are beneath the patient; the equipment above the bed is associated with targeting the stone (which may be done with ultrasound and X-rays).

The ability to correlate a given measure of biohazard (such as the cell death discussed above) with sonoluminescence allows correlation of that parameter with cavitation. Hence the presence or absence of sonoluminescence can be used as an indicator of whether or not bubble activity capable of biohazard is present. Such biohazard might be desirable in dental ultrasonics^{101,102}, where it can perform a sterilising function; but undesirable during foetal scanning¹⁰³. The only quantification to date¹⁰⁴ of collapse cavitation produced *in vivo* in humans was done through a sonoluminescence

study: Although this finding was very important, and used in international guidelines¹⁰⁵ for the safe use of ultrasound, the extreme difficulty of the experiment has meant that much-needed independent follow-on measurements have never been successfully completed.

Another example of correlating cavitation with a biophysical parameter via sonoluminescence, has led to a recent innovation in the field of lithotripsy¹⁰⁶ (Figure 16). Here, a correlation between the sonoluminescent and the passive acoustic emissions, identified cavitation as the source of that acoustic emission^{107,108}. This has led to numerous studies, and a patented device for monitoring the degree of stone fragmentation during lithotripsy¹⁰⁹ (Figure 17). Such studies have been heavily reliant on associated computational fluid dynamics^{1,110-113} (Figure 18). Although lithotripsy is in most cases far preferable to the surgical removal of kidney and gall stones, there is currently no method of monitoring the degree of stone fragmentation. As a result, patients are subjected to a preset number of shocks (several thousand). If too few are given, re-treatment is necessary. If too many shocks are given, unnecessary exposure and collateral tissue damage may occur. In addition, the expensive shock wave sources have a lifetime limited by the number of firings. The ability to limit the number of shocks to the number required for adequate stone fragmentation would conserve hospital resources, both financially and in terms of waiting times¹¹⁴.

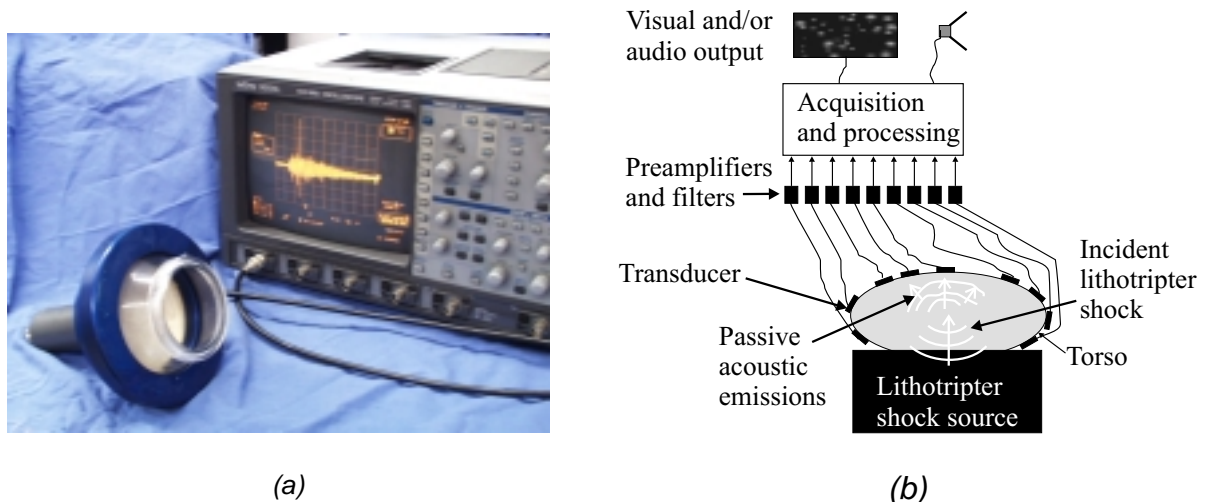


Figure 17. (a) Photograph of an early prototype passive cavitation detector, with typical cavitation emissions displayed. This device consisted of a bowl hydrophone, resonant at 1 MHz, which was placed on the patient and allowed in vivo monitoring of acoustic emissions resulting from cavitation during lithotripsy. (b) Schematic for the operation of the broadband clinical prototype¹⁰⁹ passive cavitation detector. The lithotripter focuses a shock wave onto the kidney stone from below (as in Figure 16b). Broadband sensors placed on the torso detect the passive acoustic emissions, and these are processed to give feedback to the clinician (either in audio form, or as a display) on the targeting of the lithotripter, on the cavitation which occurs in vivo, and on the degree of stone fragmentation. See Fedele et al. (this volume)¹¹⁴.

In the above examples, processing took place through jet impact, and blast waves, and chemical effects when compressed gas within the collapsing bubble attains temperatures in excess of 6000 K (the temperature of the surface of the sun), and generates highly reactive chemical species. These effects are characteristic of inertial (or transient¹¹⁵) cavitation, and hence require acoustic pressure amplitudes greater than 100 kPa. Not all processing requires this, and indeed the discovery that processing can take place with acoustic pressure amplitudes of 100 Pa opens up not only the new field of acoustoelectrochemistry¹¹⁶⁻¹²¹, but also the possibility that significant future savings might be made by the ultrasonic processing industry in their power requirements. In addition, it opens up an exciting new fields of study, for example in the chaotic growth^{122,123} of surface waves on bubble walls (Figures 19 and 20).

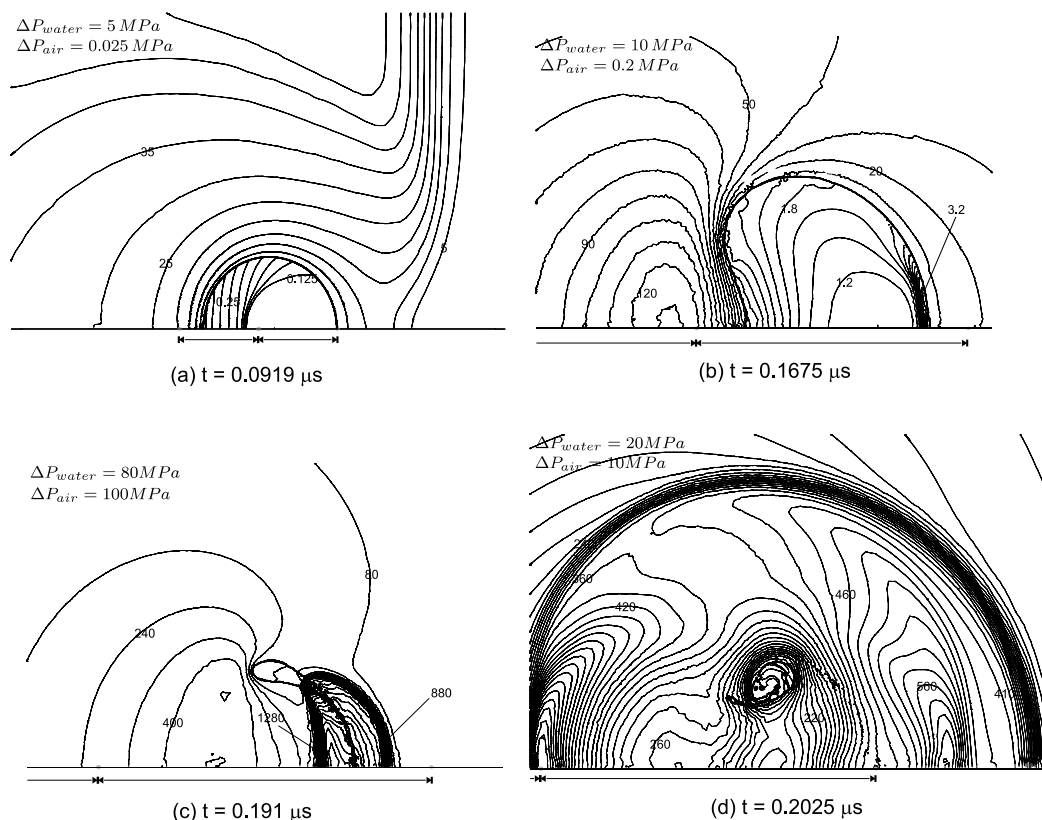
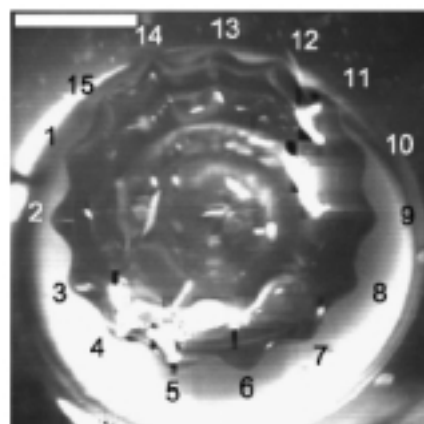


Figure 18. An air bubble of initial radius 40 microns in water is subjected in the free field to a lithotripter pulse (propagating from left to right). The response is predicted by the Vucalm hydrocode, the axis of rotational symmetry being the horizontal line at the base of each plot. The contour increments in pressure for both air and water are indicated on each plot, the value of selected contours being labelled in MPa. All elapsed times 't' are measured after the lithotripter pulse first meets the upstream bubble wall. (a) The lithotripter pulse has passed over the bubble, travelling further than the slower gas shock within the bubble. An expansion wave is reflected back off the bubble, travelling to the left and upwards in the picture. (b) The bubble involutes as it collapses, to form a liquid jet which will pass through the centre of the bubble. (c) The impact of the jet against the downstream bubble wall generates a blast wave, which propagates outwards in (d). Such liquid impacts and blast waves can generate erosion and biomechanical effects. The high temperatures and pressures attained within the gas can generate chemical effects and luminescence. Image courtesy A.R. Jamaluddin, C.K. Turangan, G.J. Ball and T.G. Leighton¹.

4 THE FUTURE FOR BUBBLE ACOUSTICS

The opportunities for fundamental physical and chemical research in bubble acoustics are immense. Whilst a degree of prescience would be required to outline them, the opportunities for applied research in bubble acoustics are more obvious, given that they would be building on work is currently in the research stage. Figure 1 illustrated the ability of contrast agents to provide localised enhancement in ultrasonic images. The bubble walls of contrast agents are already engineered to provide bubble longevity. Further engineering might make the bubbles attached to specific cells, so that contrast agents injected throughout the body might accumulate at specific targets sites. This could not only enable identification of the locality of specific types of cells (e.g. tumour cells) in the body, through 'hot spots' in ultrasound images. It would also place within the locality of those cells a microbubble which could be excited to process the cell (by, for example, injecting material from within the bubble into the cell at the tip of the liquid jet which forms as the bubble collapses -- Figures 18 and 21).

Figure 19. View from below of an air bubble, restrained against buoyant rise by a glass rod, visible as the white circle 'behind' the bubble (scale bar: 2 mm). The bubble ($R_0 \sim 2.5$ mm) was driven into oscillation by an acoustic driving field. Such fields will always excite the pulsation mode, but if the bubble wall pulsation amplitude is sufficiently great, instabilities on the bubble wall grow rapidly. The mode which requires the lowest amplitude of pulsation to excite corresponds to the Faraday wave. Here, the bubble was driven at 1.297 kHz, with 83.5 Pa zero-to-peak acoustic pressure amplitude. This is enough to stimulate just the Faraday wave (the $n = 15$ spherical harmonic perturbation, annotated), and of course the breathing mode ($n = 0$).



The wall displacements associated with the breathing mode are micron-order, much smaller than the Faraday wave, which therefore gives the larger visual signal. However the acoustic emission by the bubble is dominated by the monopole breathing mode, even though the greater wall displacements of the Faraday wave generate fluid currents much larger than those resulting from the breathing mode. This can be seen in Figure 20 (Image courtesy P.R. Birkin, Y.E. Watson, T.G. Leighton)¹.

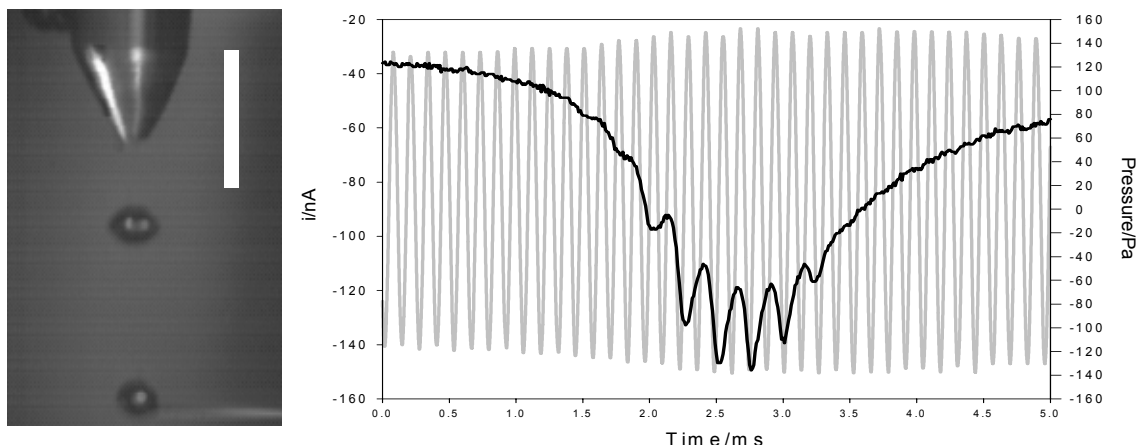


Figure 20. Bubbles are injected into a sound field, and rise under buoyancy towards an electrochemical microelectrode. In the photograph (scale bar = 2.2 mm), the horizontal injection needle can just be seen at the bottom right corner, and the downwards-facing microelectrode can be seen at the top of the picture. The microelectrode produces current as a result of mass transfer related to the presence of $5 \text{ mmol dm}^{-3} \text{ K}_3\text{Fe}(\text{CN})_6$ in $0.1 \text{ mol dm}^{-3} \text{ Sr}(\text{NO}_3)_2$, the sensing area being 25 micron diameter of Platinum at the electrode tip. Hence most of the 'microelectrode' which is visible on the photograph is the glass insulating surround. Two bubbles can be seen, the twin highlights on the upper one indicating peaks of Faraday waves (as in Figure 19). The graph shows, against a common time axis, the insonifying sound field (grey line) and the electrochemical current (black line). Flow (caused here by bubble motion, which in this experiment comprises translation, pulsation and Faraday wave) tends to disrupt the depletion layer that forms around the microelectrode tip. Therefore the current tends to increase in magnitude as the bubble moves close to the microelectrode. Such an increase is seen as the bubble approaches the needle, followed by a decrease as the bubble continues its buoyant rise above the microelectrode. At its closest approach, the current clearly shows an oscillation at the subharmonic of the driving sound field in which the Faraday waves on the bubble wall oscillate. This is of course at half of the 7.678 kHz fundamental of the driving field (grey line) at which the breathing mode oscillates. Hence the higher order mode generates a much larger electrochemical signal. (Photographs and data courtesy P.R. Birkin, Y.E. Watson, J. Flemming, T.G. Leighton)¹.

The ability of bubbles to process their environment chemically would appear to possess great potential for industry. However the commercial exploitation of these effects is limited primarily by a failure by workers to appreciate the acoustics¹²⁴⁻¹²⁹ and this has given the field the unwarranted reputation of irreproducibility and inability to scale-up. Sonochemists are in the habit of referring to their field as a "black art". It is not so, but rather it is multidisciplinary and requires in-depth appreciation of both physics and chemistry. When this is achieved, the sonochemical abilities of bubbles are understandable and could be exploited commercially.

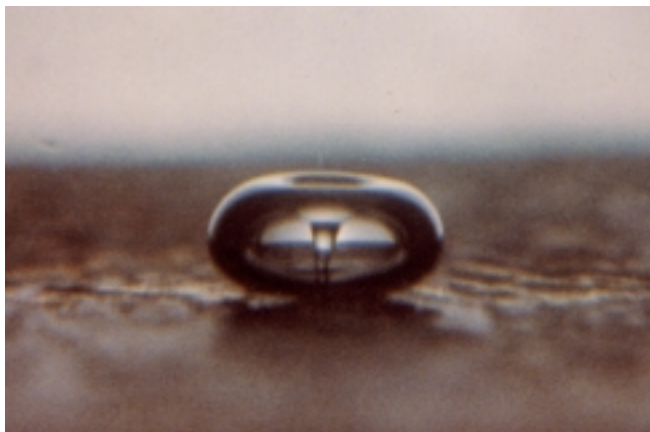


Figure 21. Jet formation during the collapse of an oscillating gas-vapour bubble at low pressure (0.04-0.05 bar) in a 60 Hz sound field. The bubble size is approximately 0.2 cm. (Photograph courtesy of LA Crum).

5 ACKNOWLEDGEMENTS

The author would like to thank the Royal Society Leverhulme Trust for a Senior Research Fellowship, and the EPSRC for research funding (GR/R12695/01, GR/S78698/01, GR/N19243/01, GR/N30989/01, GR/S01764/01). The author has made reasonable attempts to gain permission to use the images in Figures 2a, 9b, 11, 13, 16.

6 REFERENCES

1. T.G. Leighton, 'From babbling brooks to baby scans, from seas to surgeries: The pressure fields produced by non-interacting spherical bubbles at low and medium amplitudes of pulsation', *International Journal of Modern Physics B* (in preparation) (2004).
2. E.R. Hughes, T.G. Leighton, G.W. Petley and P.R. White, 'Ultrasonic propagation in cancellous bone: A new stratified model', *Ultrasound in Medicine and Biology*, 25(5), 811-821 (1999).
3. E.R. Hughes, T.G. Leighton, G.W. Petley, P.R. White and R.C. Chivers, 'Estimation of Critical and Viscous Frequencies for Biot Theory in Cancellous Bone', *Ultrasonics*, 41, 365-368 (2003).
4. E.R. Hughes, T.G. Leighton G.W. Petley and P.R. White, 'Ultrasonic Assessment of Bone Health', *Acoustics Bulletin* 26(5), 17-23, (2001).
5. T.G. Leighton (editor), 'Natural Physical Processes Associated With Sea Surface', (publ. University of Southampton), (1997).
6. T.G. Leighton, G.J. Heald, H. Griffiths and G. Griffiths (editors), 'Acoustical Oceanography, Proceedings of the Institute of Acoustics', Vol. 23 Part 2, (Bath University Press) (2001).
7. W. Munk and A.B. Baggeroer, 'The Heard Island Papers: A contribution to global acoustics', *J. Acoust. Soc. Am.*, 96, 2327-2329 (1994).
8. S.D. Richards and T.G. Leighton, 'Acoustic sensor performance in coastal waters: solid suspensions and bubbles', in 'Acoustical Oceanography', *Proceedings of the Institute of Acoustics* Vol. 23 Part 2, T.G. Leighton, G.J. Heald, H. Griffiths and G. Griffiths, (eds.), Institute of Acoustics, pp. 399-406 (2001).

9. S.D. Richards, T.G. Leighton and N.R. Brown 'Visco-inertial absorption in dilute suspensions of irregular particles'. *Proceedings of the Royal Society Series A*, 459, 1-15, 2003.
10. N.R. Brown, T.G. Leighton, S.D. Richards and A.D. Heathershaw, 'Boundary and volume losses in a diffuse acoustic field near the atmosphere/ocean boundary', *Natural Physical Processes Associated With Surface Sound* T. G. Leighton, ed., (University of Southampton) 123-132 (1997).
11. N.R. Brown, T.G. Leighton, S.D. Richards and A.D. Heathershaw, 'Measurement of viscous sound absorption at 50-150 kHz in a model turbid environment', *Journal of the Acoustical Society of America*, 104(4), 2114-2120, (1998).
12. S.D. Richards and T.G. Leighton 'High frequency sonar performance predictions for littoral operations – The effect of suspended sediments and microbubbles', *Journal of Defence Science*, 8(1), 1-7 (2003).
13. S.D. Richards, T.G. Leighton and N.R. Brown, 'Sound absorption by suspensions of nonspherical particles: Measurements compared with predictions using various particle sizing techniques', *Journal of the Acoustical Society of America*, 114(4), Pt.1, 1841-1850, (2003).
14. S.D. Richards and T.G. Leighton 'Sonar performance in coastal environments: suspended sediments and microbubbles', *Acoustics Bulletin* 26(1), 10-17, (2001).
15. S.D. Richards, Underwater acoustics and sonar performance in turbid environments, *Proceedings of the Institute of Acoustics* (this volume) (2004).
16. R. Brothers, S. Page, G.J. Heald, T.G. Leighton, M.D. Simpson and J.K. Dix, 'Analysis of very high frequency propagation in sediments: Experimental results and modelling', *J. Acoust. Soc. Am.*, 112, no. 5 Pt. 2, 2394 (2003).
17. T.G. Leighton and G.J. Heald, Chapter 21: 'Very high frequency coastal acoustic', In: *Acoustical Oceanography: Sound in the Sea* (Cambridge University Press) (H. Medwin, editor).
18. M. Gutowski, J. Bull, J.K. Dix, T. Henstock, P. Hogarth, P.R. White and T.G. Leighton, 'Chirp sub-bottom profiler source signature design and testing', *Geophysical Research Abstracts*, Volume 5, European Geophysical Society / American Geophysical Union / European Union of Geosciences Joint Assembly (in press) (2003).
19. G. Robb, A.I. Best, J.K. Dix, T.G. Leighton, A. Harris, J.S. Riggs, J.M. Bull and P.R. White, 'Frequency dependence of acoustic waves in marine sediments', *Proceedings of the Sixth European Conference on Underwater Acoustics* (ECUA'2002, 24-27 June 2002, Gdansk, Poland), (A. Stepnowski, R. Salamon and A. Partyka, eds.) 43-48, 2002.
20. J.K. Dix, S. Arnott, A.I. Best and D. Gregory, 'The acoustic characteristics of marine archaeological wood', in '*Acoustical Oceanography*', *Proceedings of the Institute of Acoustics* Vol. 23 Part 2, T. G. Leighton, G. J. Heald , H. Griffiths and G. Griffiths, (eds.), Institute of Acoustics, pp. 299-305 (2001).
21. J. M. Smith, 'Coastal Engineering 2002 Solving Coastal Conundrums', (In 3 Volumes) *Proceedings of the 28th International Conference* (World Scientific, 2002).
22. D.H. Peregrine, 'Breaking Waves on Beaches', *Ann. Rev. Fluid Mech.*, 15, 149-178 (1983).
23. M.S. Longuet-Higgins, J.S. Turner, 'An "entraining plume" model of a spilling breaker', *J. Fluid Mech.*, 63:1-20, (1974).
24. M.S. Longuet-Higgins, 'Bubble noise spectra', *J. Acoust. Soc. Am.* 87(2): 652-661, (1990).
25. D.H. Peregrine, 'Water-wave impact on walls', *Annual Review of Fluid Mechanics*, 35, 23-43, (2003).
26. I. Leifer, and A.G. Judd, 'Oceanic methane layers: the hydrocarbon seep bubble deposition hypothesis', *Terra Nova* 14 (6), 417-424, (2002).
27. P.S. Liss, and R.A. Duce, (Editors) '*The Sea Surface and Global Change*', Cambridge University Press, (1997).
28. I. Anderson, and S. Bowler, 'Oceans spring surprise on climate modellers', *New Scientist*, 125: 1707 (1990).
29. Lord Rayleigh, 'On the pressure developed in a liquid during the collapse of a spherical cavity', *Phil. Mag.*, 34, 94-98 (1917).

-
30. T.G. Leighton and A.J. Walton, 'An experimental study of the sound emitted from gas bubbles in a liquid', *European Journal of Physics*, 8, 98-104, (1987).
 31. M.R. Loewen and W.K. Melville 'A model for the sound generated by breaking waves', *J. Acoust. Soc. Am.* 90, 2075-2080, (1991).
 32. J. A. Nystuen, M. J. McPhaden, 'The beginnings of operational marine weather observations using underwater ambient sound', In '*Acoustical Oceanography*', *Proceedings of the Institute of Acoustics* Vol. 23 Part 2, T. G. Leighton, G. J. Heald, H. Griffiths and G. Griffiths, (eds.), Institute of Acoustics, 135-141 (2001).
 33. T.G. Leighton, M.F. Schneider and P.R. White, 'Study of bubble fragmentation using optical and acoustic techniques', *Sea Surface Sound '94. Proceedings of the 3rd Meeting on Natural Physical Processes related to Sea Surface Sound*, M.J. Buckingham, J. R. Potter, eds., (World Scientific Publishing Ltd., Singapore) 414-428, (1995).
 34. T.G. Leighton, K.J. Fagan and J.E. Field, 'Acoustic and photographic studies of injected bubbles', *European Journal of Physics*, 12, 77-85, (1991).
 35. T.G. Leighton, P.R. White and M.F. Schneider, 'The detection and dimension of bubble entrainment and comminution', *Journal of the Acoustical Society of America*, 103(4), 1825-1835 (1998).
 36. T.G. Leighton, *The Acoustic Bubble*, Academic Press. (1994).
 37. M.S. Longuet-Higgins 'Monopole emission of sound by asymmetric bubble oscillations', Part 1. Normal modes. *J. Fluid Mech.*, 201:525-541 (1989).
 38. M.S. Longuet-Higgins, 'Monopole emission of sound by asymmetric bubble oscillations', Part 2. An initial value problem. *J. Fluid Mech.*, 201:543-565 (1989).
 39. M.S. Longuet-Higgins, 'Resonance in nonlinear bubble oscillations', *J. Fluid Mech.*, 224:531-549, (1991).
 40. M.S. Longuet-Higgins, 'Nonlinear damping of bubble oscillations by resonant interaction', *J. Acoust. Soc. Am.*, 91: 1414-1422, (1992).
 41. M.J. Buckingham and C.L. Epifanio, 'Bubbles and breaking waves: Imaging in space, time and frequency', *Natural Physical Processes Associated With Sea Surface*, T.G. Leighton, editor (publ. University of Southampton), 39-44, (1997).
 42. M.L. Denbow, A.W. Welsh, J.M. Taylor, M.J.K. Blomley, FRCR, D.O. Cosgrove and N.M. Fisk, 'Twin Fetuses: Intravascular Microbubble US Contrast Agent Administration-Early Experience', *Radiology*, 214:724-728 (2000).
 43. T.G. Leighton, 'Acoustic Bubble Detection. I. The detection of stable gas bodies', *Environmental Engineering*, 7, 9-16, (1994).
 44. T.G. Leighton, P.R. White and M.A. Marsden, 'The one-dimensional bubble: An unusual oscillator, with applications to human bioeffects of underwater sound', *European Journal of Physics*, 16, 275-281, (1995).
 45. T.G. Leighton, P.R. White and M.A. Marsden, 'Applications of one-dimensional bubbles to lithotripsy, and to diver response to low frequency sound', *Acta Acustica*, 3, 517-529, (1995).
 46. T.G. Leighton, D.G. Ramble, A.D. Phelps, C.L. Morfey and P.P. Harris, 'Acoustic detection of gas bubbles in a pipe', *Acta Acustica*, 84, 801-814, (1998).
 47. T.G. Leighton, P.R. White P.R. C.L. Morfey, J.W.L. Clarke, G.J. Heald, H.A. Dumbrell and K.R. Holland, 'The effect of reverberation on the damping of bubbles', *Journal of the Acoustical Society of America*, 112(4), 1366-1376 (2002).
 48. R.C. Evans and T.G. Leighton, 'An experimental investigation of acoustic penetration into sandy sediments at sub-critical grazing angles', *Proceedings of the 4th European Conference on Underwater Acoustics, Rome* (ed. A. Alippi, G. B. Cannellii), 697-702, (1998).
 49. R.C. Evans and T.G. Leighton, 'The detection of cylindrical objects of low acoustic contrast buried in the seabed', *Proceedings of the Joint meeting of the 16th International Congress on Acoustics and the 135th Meeting of the Acoustical Society of America*, P. K. Kuhl, L .A. Crum, ed., (Acoustical Society of America) 1369-1370 (1998).

-
50. T.G. Leighton, A.D. Phelps and D.G. Ramble, The 1994 A. B. Wood Medal Address – ‘Acoustic bubble sizing: from laboratory to the surf zone trials’, *Acoustic Bulletin*, 21, 5-12, (1996).
 51. A.D. Phelps and T.G. Leighton, ‘Oceanic bubble population measurements using a buoy-deployed combination frequency technique’, *IEEE Journal of Oceanic Engineering*, 23(4), 400-410, (1998).
 52. T.G. Leighton, M.D. Simpson, S.D. Meers, P.R. White, G.J. Heald, H.A. Dumbrell, J.W. Clarke, P.R. Birkin and Y. Watson, ‘Surf-zone bubble detection using multiple techniques: The Worbarrow Bay experiment’, *J. Acoust. Soc. Am.*, 108(5), Part 2, 2493, (2000).
 53. A.D. Phelps, D.G. Ramble and T.G. Leighton, ‘The use of a combination frequency technique to measure the surf zone bubble population’, *Journal of the Acoustical Society of America*, 101(4), 1981-1989, (1997).
 54. T.G. Leighton, A.D. Phelps, D.G. Ramble and D.A. Sharpe, ‘Comparison of the abilities of eight acoustic techniques to detect and size a single bubble’, *Ultrasonics*, 34, 661-667, (1996).
 55. T.G. Leighton, D.G. Ramble and A.D. Phelps, ‘The detection of tethered and rising bubbles using multiple acoustic techniques’, *Journal of the Acoustical Society of America*, 101(5), 2626-2635, (1997).
 56. T.G. Leighton, R.J. Lingard, A.J. Walton and J.E. Field, ‘Acoustic bubble sizing by the combination of subharmonic emissions with an imaging frequency’, *Ultrasonics*, 29, 319-323, (1991).
 57. A.D. Phelps and T.G. Leighton, ‘High resolution bubble sizing through detection of the subharmonic response with a two frequency excitation technique’, *Journal of the Acoustical Society of America*, 99, 1985-1992, (1996).
 58. A.D. Phelps and T.G. Leighton, ‘The subharmonic oscillations and combination-frequency emissions from a resonant bubble: their properties and generation mechanisms’, *Acta Acustica*, 83, 59-66, (1997).
 59. T.G. Leighton and A.D. Phelps, ‘Letter on the mechanism for the generation of combination frequencies involving the subharmonic of the bubble resonance’, *Ultrasonics*, 35, 183, (1997).
 60. P.R. White, W.B. Collis, T.G. Leighton and J.K. Hammond, ‘Detection of bubbles via Higher Order Statistics’, *Natural Physical Processes Associated With Surface Sound*. T G Leighton, ed., (University of Southampton) 179-185 (1997).
 61. P.R. White, W.B. Collis and T.G. Leighton, ‘Analysis of bubble scattering data using higher order statistics’, *Proceedings of the 3rd European Conference on Underwater Acoustics, Heraklion* (ed. J. Papadakis), 1155-1160, (1996).
 62. P.R. White, and T.G. Leighton, ‘Passive Estimation of Bubble Size Distributions using Higher Order Statistics’, *Proceedings of the Institute of Acoustics International Conference on Sonar Signal Processing* (in press) (2004).
 63. P.R. White, and T.G. Leighton, ‘Exploitation of higher order statistics to compute density of bubble clouds; evading Olber’s paradox’, *Proceedings of the Seventh European Conference on Underwater Acoustics* (in press) (2004).
 64. P.R. Birkin, Y.E. Watson, K.L. Smith, T.G. Leighton and M.D. Simpson, ‘Measurement of species flux from a bubble using an acousto-electrochemical technique’, in ‘*Acoustical Oceanography*’, *Proceedings of the Institute of Acoustics* Vol. 23 Part 2, T. G. Leighton, G. J. Heald, H. Griffiths and G. Griffiths, (eds.), Institute of Acoustics, pp. 242-249, (2001).
 65. T.G. Leighton, S.D. Meers, M.D. Simpson, J.W.L. Clarke, G.T. Yim, P.R. Birkin, Y. Watson, P.R. White, G.J. Heald, H.A. Dumbrell, R.L. Culver, and S.D. Richards, ‘The Hurst Spit experiment: The characterization of bubbles in the surf zone using multiple acoustic techniques’, in ‘*Acoustical Oceanography*’, *Proceedings of the Institute of Acoustics* Vol. 23 Part 2, T G Leighton, G J Heald, H Griffiths and G Griffiths, (eds.), Institute of Acoustics, pp. 227-234, (2001).
 66. T.G. Leighton, A.D. Phelps and D.G. Ramble, ‘Bubble detection using low amplitude multiple acoustic techniques’, *Proceedings of the 3rd European Conference on Underwater Acoustics, Heraklion* (ed. J. Papadakis), 1143-1147, (1996).

-
67. T.G. Leighton, The Inaugural Medwin Award Address – ‘Surf zone bubble spectrometry: The role of the acoustic cross section’, *J. Acoust. Soc. Am.*, 110(5) Part 2, 2694, (2001).
 68. K.W. Commander and R.J. McDonald, ‘Finite-element solution of the inverse problem in bubble swarm acoustics’, *J. Acoust. Soc. Am.* 89(2), 592-597, (1991).
 69. T.G. Leighton, ‘Fundamentals of Underwater Acoustics and Ultrasound,’ Chapter 7 in Volume 1, *In: ed. F. J. Fahy and J. G. Walker, Noise and Vibration*, E & F Spon (an imprint of Routledge, London), 373-444, (1998).
 70. T.G. Leighton, S.D. Richards and P.R. White, ‘Trapped within a ‘wall of sound’: A possible mechanism for the bubble nets of humpback whales’, *Acoustics Bulletin* 29, 24-29 (2004).
 71. H. Williams, *Whale Nation*, Jonathan Cape (London), (1988).
 72. Sharpe, F. A., and Dill, L. M., *Canadian Journal of Zoology-Revue Canadienne de Zoologie* **75**, 725-730 (1997).
 73. Examples available at
<http://www.groovedwhale.com>;
<http://www.sfu.ca/biology/berg/whale/abcwhale.html>;
<http://students.ceid.upatras.gr/~pirli/whales/whales.html>;
 74. F.B. Jensen, W.A. Kuperman, M.B. Porter and H. Schmidt, *Computational Ocean Acoustics*. Springer-Verlag (New York) (2000).
 75. L.N. Frazer and E. Mercado, ‘A sonar model for humpback whale song’, *IEEE J. Oceanic Engineering*, **25**(1), 160-182 (2000).
 76. E. Mercado and L.N. Frazer, ‘Humpback whale song or humpback whale sonar –a reply to Au *et al.*’, *IEEE J. Oceanic Engineering*, **26**(3), 406-415 (2001).
 77. C. Levenson, ‘Characteristics of sound produced by humpback whales (*Megaptera novaeangliae*)’, in *NAVOCEANO Technical Note 7700-6-72*. Washington, DC: Naval Oceanographic Office (1972).
 78. W.W.L. Au, A.A. Pack, M.O. Lammers, L. Herman, K. Andrews and M. Deakos, ‘The acoustic field of singing humpback whales in the vertical plane’, *J. Acoust. Soc. Am.*, 113, 2277 (2003).
 79. W. Au, D. James, and K. Andrews, ‘High-frequency harmonics and source level of humpback whale songs’, *J. Acoust. Soc. Am.*, 110, 2770 (2001).
 80. A. Byatt, A. Fothergill, M. Holmes and Sir D. Attenborough, ‘The Blue Planet’, BBC Consumer Publishing (2001).
 81. K.W. Commander, A. Prosperetti, ‘Linear pressure waves in bubbly liquids: Comparison between theory and experiments’, *J. Acoust. Soc. Am.* 85: 732-746, (1989).
 82. T.G. Leighton, M. Wilkinson, A.J. Walton and J.E. Field, ‘The forced oscillations of bubbles in a simulated acoustic field’, *European Journal of Physics*, 11, 352-358, (1990).
 83. T.G. Leighton, S.D. Meers and P.R. White, ‘Propagation through nonlinear time-dependent bubble clouds, and the estimation of bubble populations from measured acoustic characteristics’, *Proceedings of the Royal Society* (in press) (2004).
 84. J.W.L. Clarke and T.G. Leighton, ‘A method for estimating time-dependent acoustic cross-sections of bubbles and bubble clouds prior to the steady state’, *J. Acoust. Soc. Am.*, 107(4), 1922-1929 (2000).
 85. S.D. Meers, T.G. Leighton, J.W.L. Clarke, G.J. Heald, H.A. Dumbrell and P.R. White, ‘The importance of bubble ring-up and pulse length in estimating the bubble distribution from propagation measurements’, in ‘*Acoustical Oceanography*’, *Proceedings of the Institute of Acoustics* Vol. 23 Part 2, T.G. Leighton, G.J Heald, H. Griffiths and G. Griffiths, (eds.), Institute of Acoustics, pp. 235-241, (2001).
 86. T.G. Leighton, ‘Nonlinear Bubble Dynamics And The Effects On Propagation Through Near-Surface Bubble Layers, High-Frequency Ocean Acoustics’, Eds. M.B. Porter, M. Siderius, and W. Kuperman, 2005, American Institute of Physics, Melville, New York (in press) (2004).
 87. B. Zeqiri, M. Hodnett and T.G. Leighton, ‘A strategy for the development and standardisation of measurement methods for high power/cavitating ultrasonic fields’, – Final project report. *NPL Report CIRA(EXT)016 for National Measurement System Policy Unit (Department of Trade and Industry)*, (January 1997).

-
88. T.G. Leighton, M. Farhat, J.E. Field and F. Avellan, 'Cavitation luminescence from flow over a hydrofoil in a cavitation tunnel', *J. Fluid Mech.*, 480, 43-60, (2003).
 89. T.G. Leighton, W.L. Ho and R. Flaxman, 'Sonoluminescence from the unstable collapse of a conical bubble', *Ultrasonics*, 35, 399-405 (1997).
 90. T.G. Leighton, A.D. Phelps, B.T. Cox and W.L. Ho, 'Theory and preliminary measurements of the Rayleigh-like collapse of a conical bubble', *Acta Acustica*, 84(6), 1014-1024, (1998).
 91. T.G. Leighton, B.T. Cox and A.D. Phelps, 'The Rayleigh-like collapse of a conical bubble', *Journal of the Acoustical Society of America*, 107(1), 130-142 (2000).
 92. T.G. Leighton, B.T. Cox, P.R. Birkin and T. Bayliss, 'The Rayleigh-like collapse of a conical bubble: Measurements of meniscus, liquid pressure, and electrochemistry', *Proceedings of the 137th Regular Meeting of the Acoustical Society of America and the 2nd Convention of the European Acoustics Association (Forum Acusticum 99, integrating the 25th German Acoustics DAGA Conference)*, Paper 3APAB_1 (March 1999).
 93. T.G. Leighton, M.J.W. Pickworth, A.J. Walton and P.P. Dendy, 'Studies of the cavitation effects of clinical ultrasound by sonoluminescence: 1. Correlation of sonoluminescence with the standing-wave pattern in an acoustic field produced by a therapeutic unit', *Physics in Medicine and Biology*, 33 (11), 1239-1248 (1988).
 94. M.J.W. Pickworth, P.P. Dendy, P.R. Twentyman and T.G. Leighton, 'Studies of the cavitation effects of clinical ultrasound by sonoluminescence: 4. The effect of therapeutic ultrasound on cells in monolayer culture in a standing wave field', *Physics in Medicine and Biology*, 34 (11), 1553-1560 (1989).
 95. T.G. Leighton, A.J. Walton and M.J.W. Pickworth, 'Primary Bjerknes Forces', *European Journal of Physics.*, 11, 47-50 (1990).
 96. M.J.W. Pickworth, P.P. Dendy, T.G. Leighton and A.J. Walton, 'Studies of the cavitation effects of clinical ultrasound by sonoluminescence: 2. Thresholds for sonoluminescence from a therapeutic ultrasound beam and the effect of temperature and duty cycle', *Physics in Medicine and Biology*, 33 (11), 1249-1260 (1988).
 97. M.J.W. Pickworth, P.P. Dendy, T.G. Leighton and E. Worpe, 'Cavitation from pulses of a few microseconds duration', *Physics in Medicine and Biology*, 34 (1), 135-136, (1989).
 98. M.J.W. Pickworth, P.P. Dendy, T.G. Leighton, E. Worpe and R.C. Chivers, 'Studies of the cavitation effects of clinical ultrasound by sonoluminescence. 3: Cavitation from pulses a few microseconds in length', *Physics in Medicine and Biology*, 34 (9), 1139-1151 (1989).
 99. T.G. Leighton, 'Transient excitation of insonated bubbles', *Ultrasonics*, 27(1), 50-53 (1989).
 100. T.G. Leighton, A.J. Walton and J.E. Field, 'High-speed photography of transient excitation', *Ultrasonics*, 27, 370-373 (1989).
 101. R. O'Leary, A.M. Sved, E.H. Davies, T.G. Leighton, M. Wilson and J.B. Kieser, 'The bactericidal effects of dental ultrasound on *Actinobacillus actinomycetemcomitans* and *Porphyromonas gingivalis* - An *in vitro* investigation', *Journal of Clinical Periodonol.* 24, 432-439 (1997).
 102. R. O'Leary, A.M. Sved, E.H. Davies, T.G. Leighton, M. Wilson and J.B. Kieser, 'The bactericidal effects of dental ultrasound' *in vitro*. *Journal of Dental Research*, 74, 88. (1995).
 103. W.L. Nyborg, T.G. Leighton, D. Miller, A.J. Coleman and Y. Takeuchi, Chapter 2. 'Nonthermal issues: Cavitation - Its nature, detection and measurement', In *World Federation for Ultrasound In Medicine and Biology, Task Group Report for Safety Committee of the WFUMB: Conclusions and recommendations on thermal and non-thermal mechanisms for biological effects of ultrasound* (ed. S Barnett). *Ultrasound in Medicine and Biology*, 24, S11-S21, (1998).
 104. T.G. Leighton, M.J.W. Pickworth, J. Tudor and P.P. Dendy, 'Studies of the cavitation effects of clinical ultrasound by sonoluminescence: 5', Search for sonoluminescence *in vivo* in the human cheek, *Ultrasonics*, 28, 181-184 (1990).
 105. S. Barnett *et al.* 'World Federation for Ultrasound In Medicine and Biology, Task Group Report for Safety Committee of the WFUMB: Conclusions and recommendations on thermal and non-thermal mechanisms for biological effects of ultrasound', *Ultrasound in Medicine and Biology*, 24, S11-S21, (1998).

-
106. K.B. Cunningham, A. Coleman, T.G. Leighton and P.R. White, 'Characterising in vivo acoustic cavitation during lithotripsy with time-frequency methods', *Acoustics Bulletin* 26(5), 10-16, (2001).
 107. A.J. Coleman, M.J. Choi, J.E. Saunders and T.G. Leighton, 'Acoustic emission and sonoluminescence due to cavitation at the beam focus of an electrohydraulic shock wave lithotripter', *Ultrasound in Medicine and Biology*, 18, 267-281 (1992).
 108. A.J. Coleman, M. Whitlock, T.G. Leighton and J.E. Saunders, 'The spatial distribution of cavitation induced acoustic emission, sonoluminescence and cell lysis in the field of a shock wave lithotripter', *Physics in Medicine and Biology*, 38, 1545-1560 (1993).
 109. T.G. Leighton, A.J. Coleman, F. Fedele and P.R. White, 'A passive acoustic system for evaluating the in vivo performance of extracorporeal shock wave lithotripsy', *UK Patent Application No. 0319863.7*.
 110. A.R. Jamaluddin, G.J. Ball and T.G. Leighton, 'Free-Lagrange simulations of shock/bubble interaction in shock wave lithotripsy', Proceedings of the Second International Conference on Computational Fluid Dynamics, ICCFD, Sydney, Australia, 541-546 (15-19 July 2002).
 111. G.J. Ball, B.P. Howell, T.G. Leighton and M.J. Schofield, 'Shock-induced collapse of a cylindrical air cavity in water: a Free-Lagrange simulation', *The 22nd International Symposium on Shock Waves, London, Paper 0060*, published April 2000, 1363-1368, (July 1999).
 112. G.J. Ball, B. Howell, T.G. Leighton and M. Schofield, 'Shock-induced collapse of a cylindrical air cavity in water: a Free-Lagrange simulation', *Shock Waves* 10, 265-276 (2000).
 113. A.R. Jamaluddin, G.J. Ball and T.G. Leighton, 'Free-Lagrange simulations of shock/bubble interaction in shock wave lithotripsy', *The 24th International Symposium on Shock Waves, Beijing, China (in press) (July 20-25, 2003)*.
 114. F. Fedele, A.J. Coleman, T.G. Leighton and P.R. White, 'A new sensor for detecting and characterising acoustic cavitation in vivo during ESWL', Proceedings of the Institute of Acoustics (this volume) (2004).
 115. T.G. Leighton, 'Acoustic Bubble Detection. II. The detection of transient cavitation', *Environmental Engineering*, 8, 16-25 (1995).
 116. P.R. Birkin, T.G. Leighton and Y.E. Watson, 'The use of Acoustoelectrochemistry to investigate bubble phenomena – Rectified diffusion', Proceedings of the Fourth International Conference on 'Applications of Power Ultrasound in Physical and Chemical Processing' (Beasancon) 101-106 (2003).
 117. P.R. Birkin, Y.E. Watson, T.G. Leighton and K.L. Smith 'Electrochemical detection of Faraday waves on the surface of a gas bubble', *Langmuir Surfaces and Colloids*, 18, 2135-2140 (2002).
 118. P.R. Birkin, Y.E. Watson and T.G. Leighton, 'Efficient mass transfer from an acoustically oscillated gas bubble', *J. Chem. Soc. Chemical Communications*, 24, 2650-2651 (2001).
 119. P.R. Birkin, T.G. Leighton and Y.E. Watson, 'The use of Acoustoelectrochemistry to investigate rectified diffusion', *Ultrasonics Sonochemistry* (in press).
 120. Y.E. Watson, P.R. Birkin and T.G. Leighton, 'Electrochemical detection of bubble oscillation. *Ultrasonics*', *Sonochemistry*, 10, 2003, 65-69 (2003).
 121. P.R. Birkin, T.G. Leighton, Y.E. Watson and J.F. Power, 'Acoustoelectrochemistry', *Acoustics Bulletin* 26(5), 24-37 (2001).
 122. A. Maksimov, T.G. Leighton and E.V. Sosedko, 'Nonlinear Transient Bubble Oscillations', In: *Nonlinear Acoustics at the Beginning of the 21st Century* (Proceedings of the 16th International Symposium on Nonlinear Acoustics), edited by O.V. Rudenko and O.A. Sapozhnikov vol. 2, pp. 987-990 (Faculty of Physics, MSU, Moscow, 2002).
 123. A.O. Maksimov and T.G. Leighton, 'Transient processes near the threshold of acoustically driven bubble shape oscillations', *Acta Acustica* 87(3), 322-332 (2001).
 124. T.G. Leighton, 'Bubble population phenomena in acoustic cavitation', *Ultrasonics Sonochemistry*, 2, S123-136 (1995).
 125. P.R. Birkin, T.G. Leighton, J.F. Power, M.D. Simpson, A.M.L. Vincotte and P.F. Joseph, 'Experimental and theoretical characterisation of sonochemical cells. Part 1: Cylindrical

- reactors, and their use to calculate speed of sound', *J. Phys. Chem .A*, 107, 306-320 (2003).
126. P.R. Birkin, J.F. Power, A.M.L. Vincotte and T.G. Leighton, 'A 1 kHz resolution frequency study of a variety of sonochemical processes', *Physical Chemistry Chemical Physics*, 5, 4170-4174 (2003).
127. P.R. Birkin, J.F. Power and T.G. Leighton, 'Electrochemical evidence of H• produced by ultrasound', *J. Chem. Soc. Chemical Communications*, 21, 2230-2231 (2001).
128. P.R. Birkin, J.F. Power, M.E. Abdelsalam and T.G. Leighton 'Electrochemical, luminescent and photographic characterisation of cavitation', *Ultrasonics Sonochemistry*, 10, 203-208 (2003).
129. P.R. Birkin, J.F. Power, T.G. Leighton and A.M.L. Vincotte, 'Cathodic electrochemical detection of sonochemical radical products', *Analytical Chemistry*, 74, 2584-2590 (2002).